UNIVERSITEIT VAN PRETORIA
UNIVERSITY OF PRETORIA
YUNIBESITHI YA PRETORIA

CHARACTERISATION OF TOTAL LUMINOUS FLUX MEASUREMENTS FOR LIGHT-EMITTING DIODES

by

Lindani Nicholas Tshibe

Submitted in partial fulfilment of the requirements for the degree

Master of Engineering (Electronic Engineering)

in the

Department of Electrical, Electronic and Computer Engineering
Faculty of Engineering, Built Environment and Information Technology

University of Pretoria

July 2016

SUMMARY

CHARACTERISATION OF TOTAL LUMINOUS FLUX MEASUREMENTS FOR LIGHT-EMITTING DIODES

by

Lindani Nicholas Tshibe

Supervisor: Prof. F.W. Leuschner

Department: Electrical, Electronic and Computer Engineering

University: University of Pretoria

Degree: Master of Engineering (Electronic Engineering)

Keywords: Integrating sphere, sphere-spectroradiometer, sphere-photometer, luminous flux, spectral distribution, sphere coating reflectance and absolute integrating sphere.

Light-emitting diodes (LEDs) have found a use in various applications due to their compact size, durability and energy efficiency. Traditionally, due to low levels of illuminated light, LEDs have been mostly utilised as indication lamps for signalling purposes. The introduction of high power LEDs (specifically, phosphor-based white power LEDs) has been the drive behind the replacement of traditional incandescent and fluorescent lighting applications by their LED counterparts. This is due to LEDs and other solid-state lamps (SSLs) being far more energy efficient and durable. Moreover, SSL devices can be integrated into various shapes as a luminaire, thanks to its nature of being a tiny light source in discrete form. However, the optical and electrical nature of LEDs and SSLs is different from that of traditional light sources, like incandescent lamps. These distinguishing features of LEDs sets them apart from traditional light sources and means that the treatment of LEDs (in terms of measurement) must be carefully evaluated. Variations in measurements done by manufacturers, national laboratories and end-users have been reported. Some of these discrepancies in measurements are due to temperature drifts (which is expected for an LED, as it is a semi-conductor device), their directional or spatial nature, and LEDs being narrow band sources of light (resembling laser diodes).

A method for measuring LED luminous flux has been studied and tested on a 50cm and a 200cm integrating sphere that makes use of readily available laboratory equipment. It is

demonstrated that any laboratory set-up can be individually characterised to accommodate the measurement of LEDs with controlled accuracy. Measurement traceability is transferred from a reputable national laboratory institute of South Africa (NMISA). A lumen is realised from an illuminance standard that has been tested via global inter-laboratory comparisons against other international laboratories. A lumen realised using this method also traces to an NMISA giant primary standard (an absolute radiometer).

This method eliminates the necessity of dealing with the issues that often arise when standard LED lamps are used as a reference when calibrating LED sources.

OPSOMMING

KARAKTERISERING VAN TOTALE LIGVLOED-METINGS VIR LIG-EMISSIEDIODES

deur

Lindani Nicholas Tshibe

Studieleier: Prof F.W. Leuschner

Departement: Elektriese, Elektroniese en Rekenaar-Ingenieurswese

Universiteit: Universiteit van Pretoria

Graad: Magister in Ingenieurswese (Elektroniese Ingenieurswese)

Sleutelwoorde: Integrasiegebied, sfeerspektroradiometer, sfeerfotometer, ligstroom, spektrale verspreiding, sfeerdeklaagreflektansie en absolute integrasiegebied.

Lig-emissiediodes (LEDs) word gebruik in verskeie toepassings as gevolg van hul verenigbaarheid, duursaamheid en energiedoeltreffendheid. In die verlede is LEDs meestal gebruik as aanwyserlampe vir seindoeleindes as gevolg van hulle lae verligtingsvlakke. Die ontwikkeling van hoëdrywing-LEDs (meer spesifiek, fosforgebaseerde wit LEDs) was die dryfveer vir die vervanging van konvensionele gloeilamp- en fluoresseerlampbeligting, in verskeie toepassings, deur toepaslike LEDs. Dit is omdat LEDs en ander vastetoestandligbronne (SSLs) baie meer energiedoeltreffend en duursaam is. Daarbenewens kan SSL-ligbronne gebruik word in verskeie vorms armature, omdat hulle klein bronne in kompakte vorm is. Die optiese en elektriese aard van LEDs en SSLs verskil egter van dié van konvensionele ligbronne, soos gloeilampe. Hierdie onderskeidende kenmerke van LEDs veroorsaak dat hierdie tipe ligbron heeltemal anders as konvensionele ligbronne toegepas moet word, met die gevolg dat die meting van LEDs anders hanteer en noukeurig geëvalueer moet word. Vervaardigers, nasionale laboratoriums en endgebruikers het variasies in resultate van metings deur hulle gedoen, aangemeld. Sommige van hierdie verskille is as gevolg van temperatuurdrywing (wat verwag kan word van 'n LED, omdat dit is 'n halfgeleiertoestel is), hulle gerigte of ruimtelike aard en omdat LEDs noubandligbronne kan wees (soortgelyk aan laserdiodes).

'n Metode is ondersoek en op die proef gestel op 'n 50 cm en 'n 200 cm integreersfeer onderskeidelik (wat toerusting gebruik wat geredelik beskikbaar in die laboratorium is). Daar is bevind dat enige laboratoriumopstelling individueel gekarakteriseer kan word om die meting van LEDs met akkuraatheid binne aanvaarbare toleransies te verkry. Die metingnaspeurbaarheid word oorgedra van 'n betroubare nasionale metrologie-instituut (NMISA). Die lumen word gerealiseer deur middel van 'n ligintensiteitstandaard wat geverifieer is deur middel van internasionale interlaboratoriumvergelykings met ander internasionale metrologie-institute. Tydens die lumenrealisering word daar ook naspeurbaarheid verkry na die nasionale primêre standaard soos byvoorbeeld die absolute radiometer.

Hierdie metode skakel die probleme uit wat dikwels ontstaan wanneer standaard LED-lampe as verwysing gebruik word tydens die kalibrasie van LED bronne.

ACKNOWLEDGEMENTS

The author would like to thank some of the people and organisations who were involved with this research for an MEng degree (Electronic Engineering):

- Prof. Wilhelm Leuschner, my supervisor, for providing academic guidance, motivation and encouragement.
- Miss Elsie Coetzee and Mrs Natasha Nel-Sakharova, for their guidance and availability to assist and share their expertise and knowledge in photometry.
- Miss Margaret Buzinski of the National Metrology Institute of South Africa, for the calibrated illuminance meters that were key to this project for traceability purposes.
- The National Metrology Institute of South Africa (Photometry and Radiometry department), for supporting this project by making standard equipment and calibrations available.
- Mr James Matjeke of NTL Lemnis, for providing emotional support, believing in me and making LED artefacts available for this project.
- Dr Peter Blattner of METAS (Switzerland), for supporting this research topic and for his continuous advice on the direction of the study.
- Mr Koos van der Westhuizen of Denel Aerospace, for making some of the equipment required available to take measurements during this project.
- My parents, for their continuous encouragement and for believing in me.
- Denel Land System staff, for becoming my second family.

LIST OF SYMBOLS

A	Illuminated area
d	Distance
d_o	Distance between source and detector
E	Illuminance
F	Spectral mismatch correction factor
f	Port fraction
f_1'	Photometer spectral quality index
I	Luminous intensity
L_e	Radiance
L_v	Luminance
M	Sphere multiplier
ρ	Surface reflectance
$R_s(\lambda)$	Relative throughput of an integrating sphere
sr	Steradian
$s_{cal}(\lambda)$	Spectral power distribution of a calibration source
$s_{LED}(\lambda)$	Spectral power distribution of an LED (source)
$s_{rel}(\lambda)$	Relative spectral responsivity of the sphere system
$V(\lambda)$	Luminous sensitivity of human eye
V_j	Junction voltage
Φ_v	Luminous flux

LIST OF ABBREVIATIONS

AC	Alternating current
AISM	Absolute integrating sphere method
$BaSO_4$	Barium Sulphate
BIPM	International Bureau of Weights and Measures
CCD	Charged coupled device
CCT	Correlated colour temperature
CFL	Compact fluorescent lamp
CMC	Calibration measurement capability
CRI	Colour rendering index
CIE	International Commission on Illumination
DC	Direct current
DVM	Digital voltmeter
E_{27}	27-mm Edison screw-base
FWHM	Full-width at half-maximum
LED	Light-emitting diode
LMT	Lichtmesstechnik
METAS	Federal Institute of Metrology
MU	Measurement uncertainty
NIST	National Institute of Standards and Technology
NMI	National Metrology Institute
NMISA	National Metrology Institute of South Africa
PSU	Power supply unit
RGB	Red – green – blue
SPD	Spectral power distribution
SSL	Solid-state lighting
UP	University of Pretoria

UUT	Unit under test

TABLE OF CONTENTS

CHAPTER 1 INTRODUCTION

1.1 MOTIVATION

The total luminous flux (lumen) is one of the most important characteristics of Light Emitting Diodes (LEDs), and is commonly measured using integrating sphere photometers [1, 2]. Traditionally, absolute luminous flux standard lamps have been calibrated using a goniophotometer [2], which is rather time consuming and requires sophisticated alignment of certain parts of the equipment. In place of a photometer, a spectroradiometer can also be utilised as a detector. One advantage of using a spectroradiometer is its ability to do both the intensity and spectral-based measurements. A detailed presentation on procedures and recommendations on sphere measurements based on a photometer and spectroradiometer can be found in [3, 4].

The treatment of LED lamps and modules when taking measurements is somewhat different from that of conventional sources like tungsten halogen and incandescent light sources. This is due to the complexity of the optical properties associated with LEDs. The luminous intensity and spectral power distribution of LEDs are sensitive to variations in the p-n junction temperature [5]. The spectral distribution of blue and phosphor-based white LEDs is characterised by a sharp blue peak, making LED photometric measurements more prone to error, due to imperfections on the luminosity curve $V(\lambda)$ corrected photometers, compared to cases of other conventional sources. The narrow band spectral and spatial nature of LEDs makes them susceptible to error, due to sphere surface spectral mismatch and homogeneity respectively. The LEDs come with different packages; this packaging directly affects the angular distribution of LEDs [6, 7].

While LEDs bring new possibilities to the niche field of lighting and energy management, they also come with challenges in terms of optical measurements. Accurate optical measurement of LEDs is essential in order to characterise and measure their performance against regulating standards. Due to their different optical properties from those of

conventional sources (like incandescent lamps), the methods originally developed for conventional sources may need to be modified or redesigned completely, in order to accommodate LEDs [7-10].

1.2 RESEARCH PROBLEM AND HYPOTHESIS

The problem addressed in this research is as follows:

- How would the absolute flux measurement set-up of a University of Pretoria (UP) 1.93m (76″) integrating sphere perform when characterised for measuring different LED lamps/modules?

In addressing the research question, analysis has been done regarding quantifying the relative throughput, errors created due to spectral mismatches of the sphere, opal diffuser and photometer head. The transmittance of the opal diffuser has also been evaluated.

The following is the research hypothesis:

- If all the spectral, spatial mismatches and LED junction temperature variations of the sphere-photometer measurement set-up can be quantified and corrected for, then an absolute integrating sphere method (AISM) would be more suitable for repeatable LED luminous flux measurements than relative reference sphere methods.

In order to expand on the primary research question, the following secondary research questions were addressed:

- Could the spectral response of the set-up be quantified and corrected for mismatches due to individual components? How suitable is this set-up for colour measurements?
    - Mismatches due to sphere coating and the $V(\lambda)$ filter of the photometer head all contribute to the spectral response of the system.
- How much is the total luminous flux measurement affected by the homogeneity of the integrating sphere?

  - The non-uniformity of the sphere surface and the introduction of the baffles and other components inside the sphere alter the ideal reflective environment necessary for absolute measurements to be taken.
- How does the low relative throughput of a 76″ sphere affect the linearity performance of the photometer?
  - It is expected that the performance of the set-up will be poor for LEDs with relatively lower lumen levels. These limitations have also been investigated.
- How much does the junction temperature variation affect luminous flux, spectral power distribution, and consequently the colour measurements of LEDs?
  - By constantly monitoring the ambient temperature and the junction voltage of the test source/LED, the error contribution can be corrected for.

The questions addressed here are based on making decisions in terms of the modification or redesign of sphere systems and methods, in order to accommodate LED measurements while making the smallest possible errors.

1.3 JUSTIFICATION FOR THE RESEARCH

There are different methods by which the luminous flux of LEDs can be measured. [3] recommends the use for the relative reference measurement method for LEDs. This method involves measuring the luminous flux of a test lamp against a known standard lamp. AISM was developed at the National Institute of Standards and Technology (NIST) in 1995 [11, 12] and has been tested with some modifications (using cheaper and readily available resources) at the UP, for purposes of this dissertation. These modifications have been analysed for their suitability to address LED measurement issues. The traceability of this method is based on a detector/meter standard, eliminating the uncertainties that come with aging, self-absorption issues and the uncertainties of standard lamps [13].

Due to the spectral and spatial nature of LEDs, in addition to spectral corrections, it is a requirement, for more accurate results, that the lumen standard lamp must have a spectral content and angular distribution resembling that of a test source [3, 4]. Moreover, the lumen levels should almost match those of the test source. Consequently, a number of LED lamp

standards would have to be made available in order to cater for the number of LED test sources. The uncertainty components have been compared for the conventional relative reference method [3], the AISM [11] and its modified counterpart used at UP for LED measurements, as listed in Table 1.1.

Table 1.1. Comparison of uncertainty components for different luminous flux measurement methods.

Uncertainty component	Relative reference method [3]	Absolute integrating sphere method [11]	Method proposed in this research
1) Self-absorption by the test lamp	Auxiliary lamp for correction	Eliminated in this method	Eliminated in this method
2) Near field absorption by the lamp socket/holder	High reflective coating of object surfaces required	Eliminated in this method	Eliminated in this method
3) Spectral mismatch of the integrating sphere system	UUT and standard lamp spectral performance must almost match	UUT and standard lamp can be different coloured lamps	UUT and standard lamp can be different coloured lamps
4) Effect of heat from the lamp on photometer head and sphere coating	Temperature corrected photometer	Temperature corrected photometer	Temperature corrected photometer
5) Aging of working standard lamps	Standard lamps need to be constantly monitored for performance	Eliminated in this method	Eliminated in this method
6) Uncertainty of reference standard lamps	Results highly dependent on standard lamp measurement uncertainty	Eliminated in this method	Eliminated in this method

Comparing all the uncertainty components detailed in Table 1, it is evident that it is possible to modify the absolute integrating sphere method (AISM) to accommodate LED measurements and yield better performance in terms of uncertainties.

1.4 RESEARCH METHODOLOGY

Figure 1.1 is the flow diagram depicting the research methodology that was followed in this dissertation, in order to investigate, analyse and establish a more suitable method for LED luminous flux measurements.

Primarily, all uncertainty components had to be identified, analysed and proved feasible. It is unarguable that the combined uncertainty is driven by each individual uncertainty. Therefore it is of utmost importance to analyse and understand which uncertainty components are less stringent than others, allowing the core components to be treated with care.

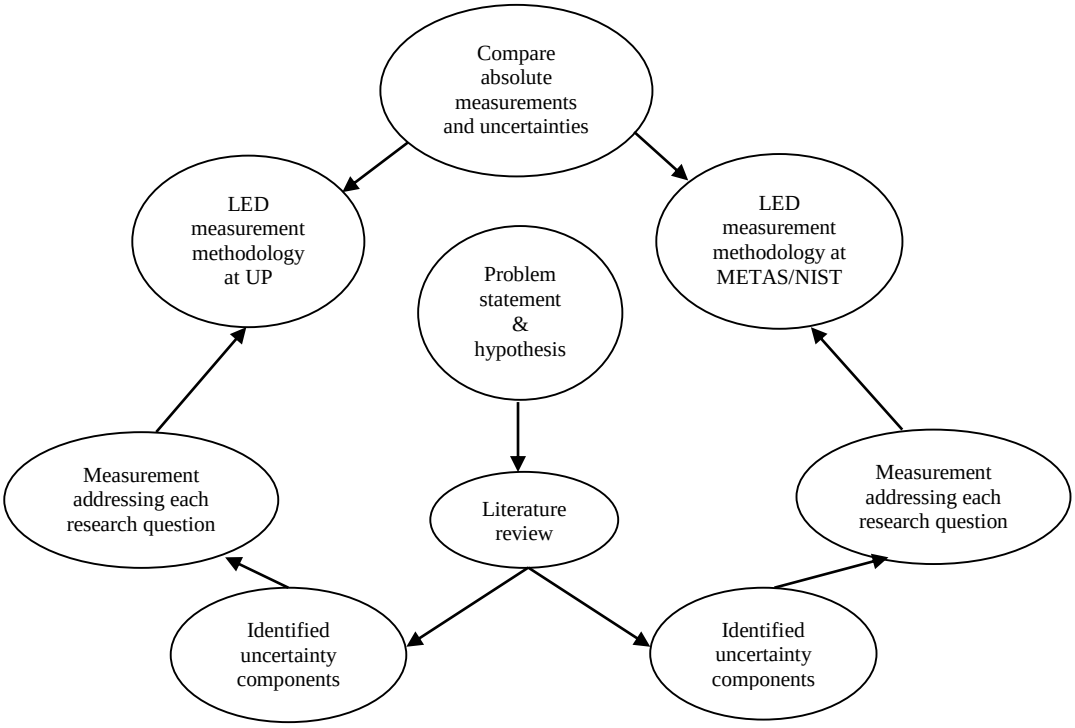

Figure 1.1. Research methodology followed in this dissertation

1.5 CONTRIBUTION OF WORK

The constant developments with solid-state lighting (SSL), especially LEDs, have placed stringent performance requirements on measurement equipment. To date, no work has been done on quantifying the performance of an integrating sphere set-up on a spectral domain using readily available photometry laboratory equipment. This dissertation is focused on bridging this research gap by introducing an approach to characterise the AISM and determine how suitable it is for taking LED luminous flux measurements without using sophisticated laboratory equipment.

1.6 ORGANISATION OF DISSERTATION

The following outlines the organisation of this dissertation:

Chapter 2 (*Literature review*)

This chapter reviews previous relevant literature and key research issues. It evaluates past contributions so that this work can be placed into context. It also highlights some of the underlying theories related to this study.

Chapter 3 (*Methodology*)

This chapter describes: the research methodology followed to develop the proposed method into a practical and sound measurement methodology; as well as the measurement set-up used to validate the measurement method.

Chapter 4 (*Measurements and results*)

This chapter presents the measurement set-up, the measurement experiments using the proposed method, and the analysis of data for correction of results.

Chapter 5 (*Discussion of measurement results*)

The results obtained in Chapter 4 and the methodology applied in this study are discussed in this chapter.

Chapter 6 (*Conclusion*)

This chapter summarises the research and hypothesis presented in this dissertation and draws concluding remarks about the work. Recommendations for future work are also presented, in line with the shortcomings of this research.

1.7 DELIMITATION OF SCOPE AND KEY ASSUMPTIONS

The delimitations applicable within the scope of work by the availability of procured equipment and time constraints for inter-laboratory comparison are given below:

- While NMISA is awaiting high-end equipment for its LED laboratory facility, this study was limited to presenting only the method and underlying bases. It is expected that the measurement uncertainties obtained will not be the best that can be obtained by the institute.
- The photometry bench at NMISA is equipped with sophisticated alignment equipment. The uncertainties obtained from UP measurements are expected to be limited in terms of measurement uncertainties due to alignment.
- Although many criteria for validating the measurement method of an institution may be acceptable, participating in an international laboratory comparison for calibration and measurement capabilities (CMCs) is the method recommended by the International Bureau of Weights and Measures (BIPM) and the CIE.

CHAPTER 2 LITERATURE REVIEW

2.1 INTRODUCTION

This chapter focuses on previous publications, with emphasis placed on the integrating sphere photometry, the fundamentals of spectral measurements and the measurement errors associated with LEDs. The discussions on these topics are not method specific, but only general photometry theories and representations.

2.2 TOTAL LUMINOUS FLUX

Total luminous flux is the fundamental quantity for a light source. It is defined as the cumulative luminous flux of a light source for the solid angle 4π Steradian (sr) [3].

The symbol of total luminous flux is Φ or Φ_v and the unit is lumen (lm). It can be calculated by the integration of luminous intensity I over the entire full solid angle Ω from the source:

$$\Phi_v = \int_0^{\Omega} I \, d\Omega \tag{2.1}$$

or, the integration of illuminance E or E_v from the source over the entire area A of a closed imaginary source surrounding a unit under test (UUT):

$$\Phi = \int_A E \, dA \tag{2.2}$$

Both Equation 2.1 and 2.2 can be applied in taking goniometric and integrating sphere measurement of the total luminous flux, respectively.

2.2.1 The integrating sphere

The light incident on a diffuse surface creates a virtual light source by reflection. The light emanating from the surface is best described by its radiance, namely the flux density per unit solid angle [14]. This quantity predicts the amount of flux that can be collected by an optical system that views the illuminated surface.

The radiance, L, of a diffuse surface for an input flux Φ_i, can be expressed as:

$$L = \frac{\Phi_i \rho}{\pi A} \qquad (\mathrm{W/m^2/sr}) \qquad (2.3)$$

where ρ is the reflectance and A is the illuminated area.

The sphere-photometer and the sphere-spectroradiometer is reportedly the quick and simplest way to measure the total luminous flux for LEDs [15, 16, and 2]. The following theory of an integrating sphere assumes the interior surface of the sphere is diffusing perfectly and has uniform reflectance throughout the sphere. Figure 2.1 shows the cross section of an integrating sphere.

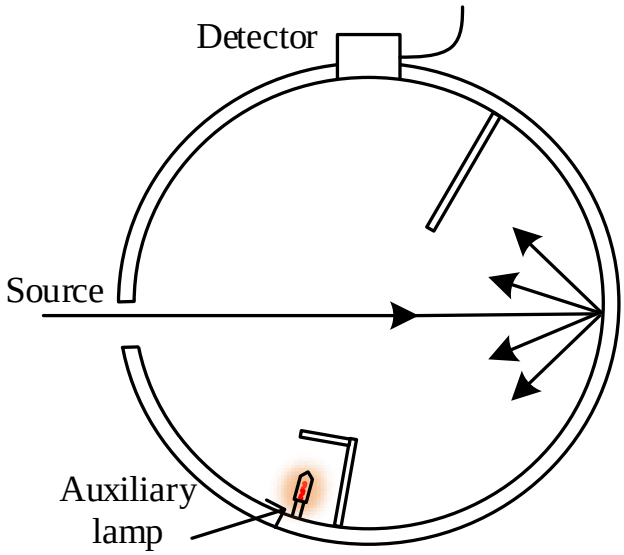

Figure 2.1. Cross section of an integrating sphere

As illustrated in Figure 2.1, the integrating sphere in general consists of the opening ports for the source under test (in the case of a 2π configuration), an auxiliary lamp and a detector head. The baffles are to prevent the detector from measuring direct light from the test source and auxiliary lamp.

Equations 2.4 to 2.10 present a summary of the integrating sphere radiance equation theory [14, 20]. The flux incident on the sphere surface is given by:

$$\Phi_1 = \Phi_i \rho \left(\frac{A_s - A_i - A_d}{A_s}\right) \tag{2.4}$$

where area components A_i, A_d and A_s are areas due to sphere openings, foreign objects (like baffles, auxiliary lamp and the test lamp) and the total surface area of an ideal sphere, respectively. The second term, in parenthesis, represents the effective flux received by the sphere and not consumed by the port openings. For simplification purposes, this term can be expressed by $(1 - f)$, where f is the port fraction, and:

$$f = \left(\frac{A_i + A_d}{A_s}\right) \tag{2.5}$$

Equation 2.4 can then be expressed as follows:

$$\Phi_1 = \Phi_i \rho (1 - f) \tag{2.6}$$

The amount of flux after the second and third reflection are:

$$\Phi_2 = \Phi_i \rho^2 (1 - f)^2 \tag{2.7}$$

And:

$$\Phi_3 = \Phi_i \rho^3 (1 - f)^3 \tag{2.8}$$

After n reflections, the total flux that is incident over the entire sphere is:

$$\Phi_T = \Phi_i \rho (1 - f) + \Phi_i \rho^2 (1 - f)^2 + \Phi_i \rho^3 (1 - f)^3 ..... + \Phi_i \rho^n (1 - f)^n \tag{2.9}$$

which can be expressed as:

$$\Phi_T = \Phi_i \rho (1 - f) \left[\sum_{n=1}^{\infty} \rho^{n-1} (1 - f)^{n-1}\right] \tag{2.10}$$

Using the infinite power series, and assuming that $r(1 - f) < 1$, this can be reduced to:

$$\Phi_T = \frac{\Phi_i \rho (1 - f)}{1 - \rho (1 - f)} \tag{2.11}$$

From Equation 2.3, the expression of radiance L_e on any given surface was presented, where A_{eff} is a total coated area of the sphere.

$$L_e = \frac{\Phi_T \rho}{\pi A_{eff}} \tag{2.12}$$

For a sphere surface, Equation 2.3 can be combined with Equation 2.11 to give:

$$L_e = \frac{\Phi_i}{\pi A_s (1-f)} \cdot \frac{\rho(1-f)}{1-\rho(1-f)} \tag{2.13}$$

By simplifying Equation 2.13 further, the sphere surface radiance is given by:

$$L_e = \frac{\Phi_i}{\pi A_s} \cdot \frac{\rho}{1-\rho(1-f)} \tag{2.14}$$

Equation 2.14 is deliberately split into two parts: the first part shows the radiance contribution due to an incoming flux onto a given surface area. It is evident that the resulting radiance at steady state is inversely proportional to the square of the sphere diameter. The second part is a unit-less contribution to the sphere, expressed by equation 2.15, known as a sphere multiplier, *M*.

$$M = \frac{\rho}{1-\rho(1-f)} \tag{2.15}$$

It can be seen in Figure 2.2 that the property *M* of an integrating sphere represents the ability of the sphere to amplify the magnitude of the incoming flux (intensity *I*).

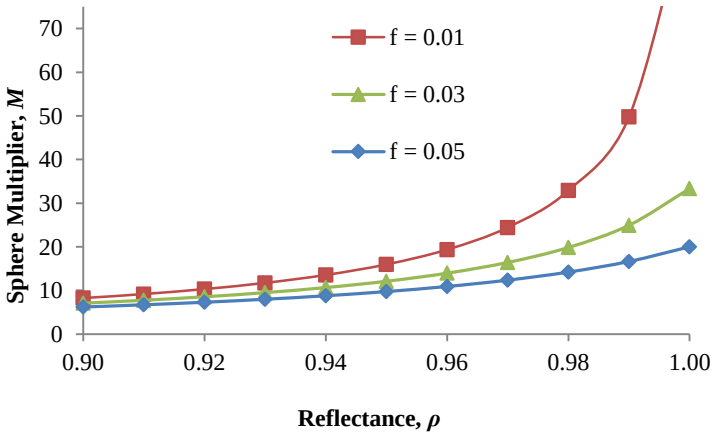

Figure 2.2. Sphere multiplier *M* as a function of sphere coating reflectance and port fraction inside the sphere

In Figure 2.2 it can be seen that for $\rho > 0.96$ and port fraction $f = \{3\%: 5\%\}$, M ranges from 10 to 30. Large spheres (larger than 1 m) typically suffer from port fraction issues due to their low f values. For national laboratory applications and any other laboratory where measurement uncertainties and minor errors are kept minimal, it is desirable for M to stay constant for as long as possible. This means that measurement results do not become very sensitive to lifespan issues, like the degradation of ρ and other LED challenges, such as measuring a test source against a dissimilar spatial distribution standard.

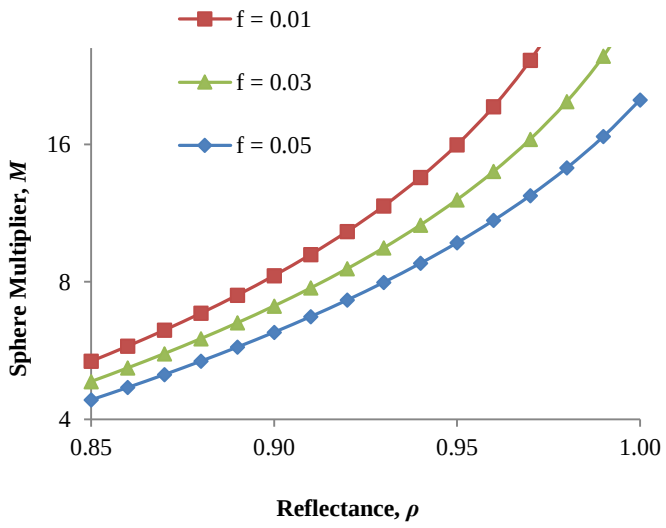

Figure 2.3. Zoomed curves of the sphere multiplier as a function of reflectance and port fraction inside the sphere

Figure 2.3 is a zoomed portion of Figure 2.2; it shows the escalated sensitivity of M for spheres with high reflective coating and good port fraction ratio. For $\rho > 0.95$, introducing a foreign object inside the sphere - hence reducing the effective area from $f = 1\%$ to $f = 5\%$ - degrades the value of the multiplier by more than 100%, while the inverse contribution due to $(1-f)$ of the first part of Equation 2.13 maybe negligible. The recommendation is therefore to carefully optimise between reflectance ρ and port reflection ratio f, especially for large integrating spheres [19].

2.2.2 Integrating sphere method of luminous flux measurements

An integrating sphere, also called an Ulbricht sphere (after the German scientist Friedrich Ulbricht), is the simplest optical device used in the measurement of luminous flux [20], amongst other purposes. The detected flux inside the integrating sphere is dependent on the input flux. The flux can be detected using a photo-detector or an optical fibre connected to a spectroradiometer. While new developments and revision of [3] are still pending, the comparison method of measurements remains a recommended method by the CIE. A test source is measured in comparison with a luminous flux standard source of known luminous flux. This method requires that many variant LEDs are calibrated for luminous flux for comparison. Other challenges associated with LEDs and comparison methods are discussed in section 2.3.

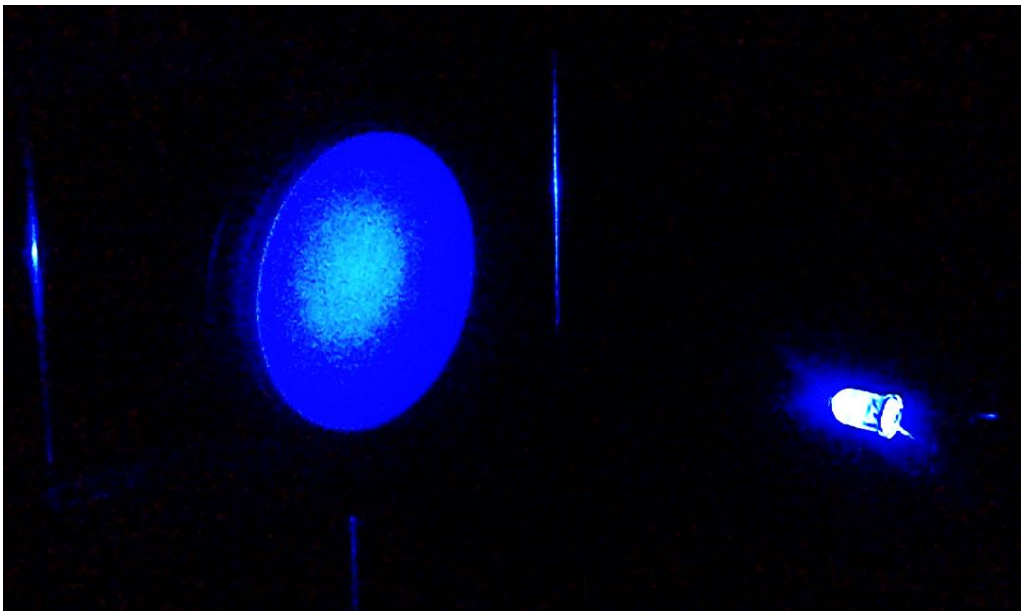

Figure 2.4. Test LED inside an integrating sphere

Figure 2.4 shows the complex radiation nature of an LED as a light. Figure 2.5 shows the recommended sphere geometries [3, 21] for total luminous flux measurements of LEDs. A 4π geometry is recommended for various LED profiles, including those with a narrow beam and those having broad and backward emissions. A 2π geometry is recommended for LEDs without backward emission (mostly high power LEDs), where the heat-sink stays outside

the sphere. This practise also avoids a steep ambient temperature gradient inside the sphere. Another advantage of a 2π geometry is the ease of mounting the lamp on the sphere wall.

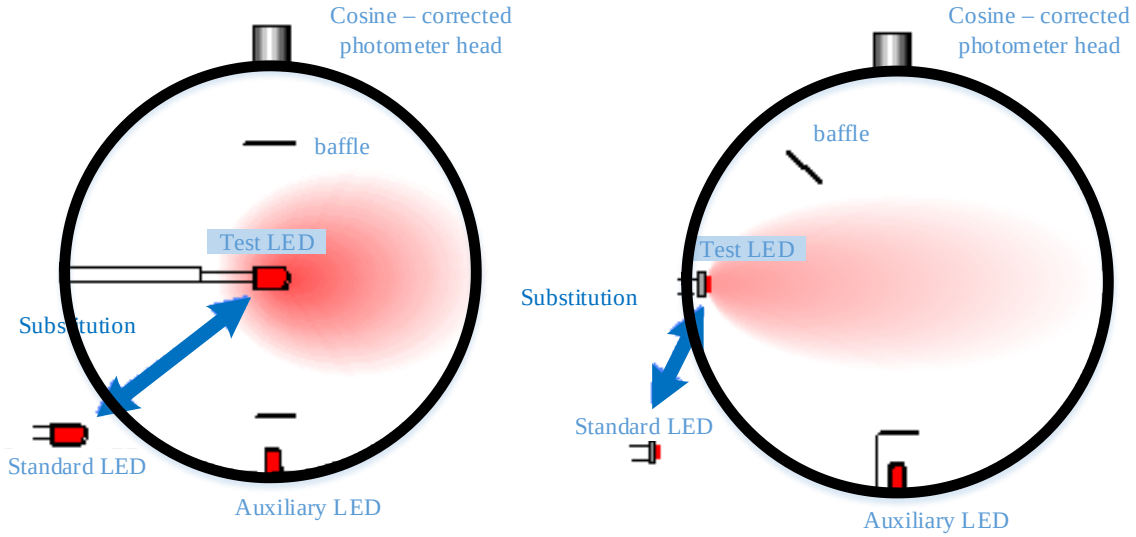

(a) (b)

Figure 2.5. Two measurement geometries for measurement of LEDs with:
(a) 4π on the left and (b) 2π radiation on the right, recommended in [3, 21]

A cosine-corrected photometer head is recommended to minimise directional errors from different angular reflections inside the sphere. It is also a CIE requirement that the photometer head $V(\lambda)$ filter must be matched to the theoretical photopic curve as accurately as possible [22, 23]. The index used to characterise the goodness of fit of the $V(\lambda)$ curve to the theoretical photopic curve is known as f_1' [24-26].

2.3 CHALLENGES WITH TAKING FLUX MEASUREMENTS

In the early years of photometry, the light was emitted by flames and glowing filaments, [27] whose spectral and spatial distributions were continuous and could be measured using straightforward methods. Discharge lamps, such as fluorescent lamps, became more attractive in general lighting because of their energy-saving characteristics and longer life-span when compared to incandescent lamps. The introduction of such lamps meant more stringent requirements [28] for flux measurements for this kind of lamp. The errors obtained when taking measurements are dependent on the quality of the $V(\lambda)$ filter match. It is evident

that with new LED sources, even bigger problems may be expected when performing such measurements.

2.3.1 Spectral content of LEDs

LEDs are quasi-monochromatic light sources. The monochromaticity of a source is measured by a quantity referred to as full-width at half-maximum (FWHM). FWHM is the width of the spectrum between the wavelengths, where the intensity has dropped by 50% from the peak intensity.

Single coloured LEDs are associated with FWHM as low as 20 nm. This makes the $V(\lambda)$ filter design more stringent, especially in the spectral regions lower than 500 nm. With white LEDs, production of white light is easily achieved in two ways. One way to achieve this is by carefully controlling the intensities of a red, green and blue (RGB) LED cluster until a white emission balance is achieved. This is called a 3-LED or RGB model. The yellow LED component can also be added for more flexibility (4-LED model) on the resultant correlated colour temperature (CCT) scale. Another way, more popular than RGB for producing white light out of the LEDs, is achieved by adding a yellowish phosphor coating. This coating is usually made of cerium doped yttrium aluminium garnet (YAG:Ce) crystals, and is added to a blue LED (usually InGaN LEDs) that has peak emission wavelengths in the region of 470 nm [29]. The blue radiation excites the yellow phosphor, which then emits a wider band light spectrum in the yellow wavelength region. The quality of the constructed white light depends mainly on the quality of the yellow phosphor, the process used and the wavelength of the blue light.

Figure 2.6 shows the spectral power distribution of three single coloured LEDs and a white LED, together with a spectrum of the CIE standard illuminant A and a $V(\lambda)$ curve.

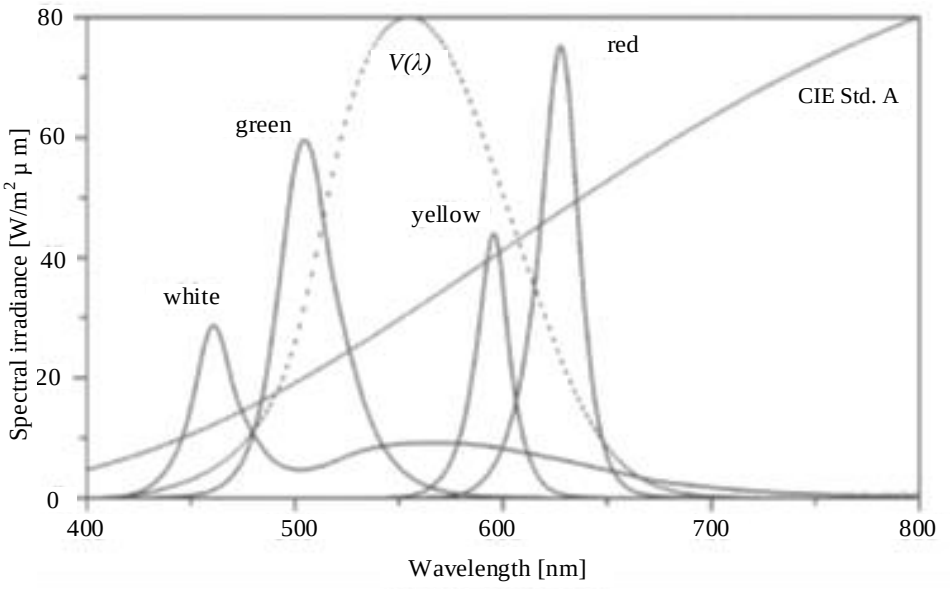

Figure 2.6. The spectral power distribution for four LEDs is illustrated with a $V(\lambda)$ curve and a spectrum of the CIE standard illuminant A

It is evident that a photometer with a slight wavelength drift from a theoretical $V(\lambda)$ around 630 nm may result in a large measurement error when measuring a red LED. The same applies to a blue LED and $V(\lambda)$ imperfections in the region of 470 nm.

Unlike in the case of traditional light sources, for comparably accurate measurements of LEDs, all the issues above need to be quantified and corrected for. The relative spectral responsivity of the measurement set-up needs to be obtained by separate measurement of the relative spectral responsivity of the photometer head [30], opal glass diffuser [31] and the relative spectral throughput of the integrating sphere [2]. The spectral quality index of a photometer is given by f'_1:

$$f_1' = \frac{\int |s^*(\lambda)_{rel} - V(\lambda)| d\lambda}{\int V(\lambda) d\lambda} \tag{2.16}$$

where $s^*(\lambda)_{rel}$ is the normalised detector responsivity.

2.3.2 Spatial luminous intensity distribution of LED sources

Unlike traditional light sources, a single LED does not emit much light [32]. In order to increase the luminous intensity of an LED, the light is often restricted to a small solid angle by making use of a lens that is integrated with an LED. A cluster of LEDs is often used where large intensities are desired (comparable to those achieved by incandescent lamps). This poses more problems: it violates most key assumptions that come with a measured source being treated as a point source [33]. LED intensities often vary even with the slightest change to the angle of observation [21]. This means that the intensity does not change uniformly with the change in solid angle. The intensity is not even symmetrical with respect to any angle in the planar view of the intensity polar plot. Measurement geometries become more challenging and some laws of optical radiation become irrelevant.

Although the above geometrical properties are discussed in the content of intensity, they also affect the total flux measurement. The measurement becomes even more prone to errors if the measuring sphere is not sufficiently homogenous.

2.4 SPECTRORADIOMETER BASED MEASUREMENTS

It is often much desirable to use a spectroradiometer in place of a photodiode to perform a luminous flux measurement when using an integrating sphere. This is usually advisable with LED measurements [34]. A spectroradiometer uses a spectrometer to separate the light from the device under test into its constituent wavelengths and to sample the spectral irradiance every nano-meter or so across a CCD array detector. From the spectral irradiance, the spectroradiometer computer program/application will accurately compute the illuminance (lux), luminous intensity (candelas), chromaticity, CCT and colour rendering index (CRI) of the device under test [35].

CHAPTER 3 METHODOLOGY

The research methodology followed in this research is described in this chapter. The method highlights the research hypothesis, analysis and validation of measurement methods. Goniometer validation (measuring from first principles) was put in place to be a secondary validation method for the hypothesis in cases where any of the selected artefacts yielded outlying/unexpected results and unacceptable spectral correction factor values for the measurement set-up.

3.1 RESEARCH METHODOLOGY OUTLINE

A research methodology is illustrated in the flow diagram shown in Figure 3.1.

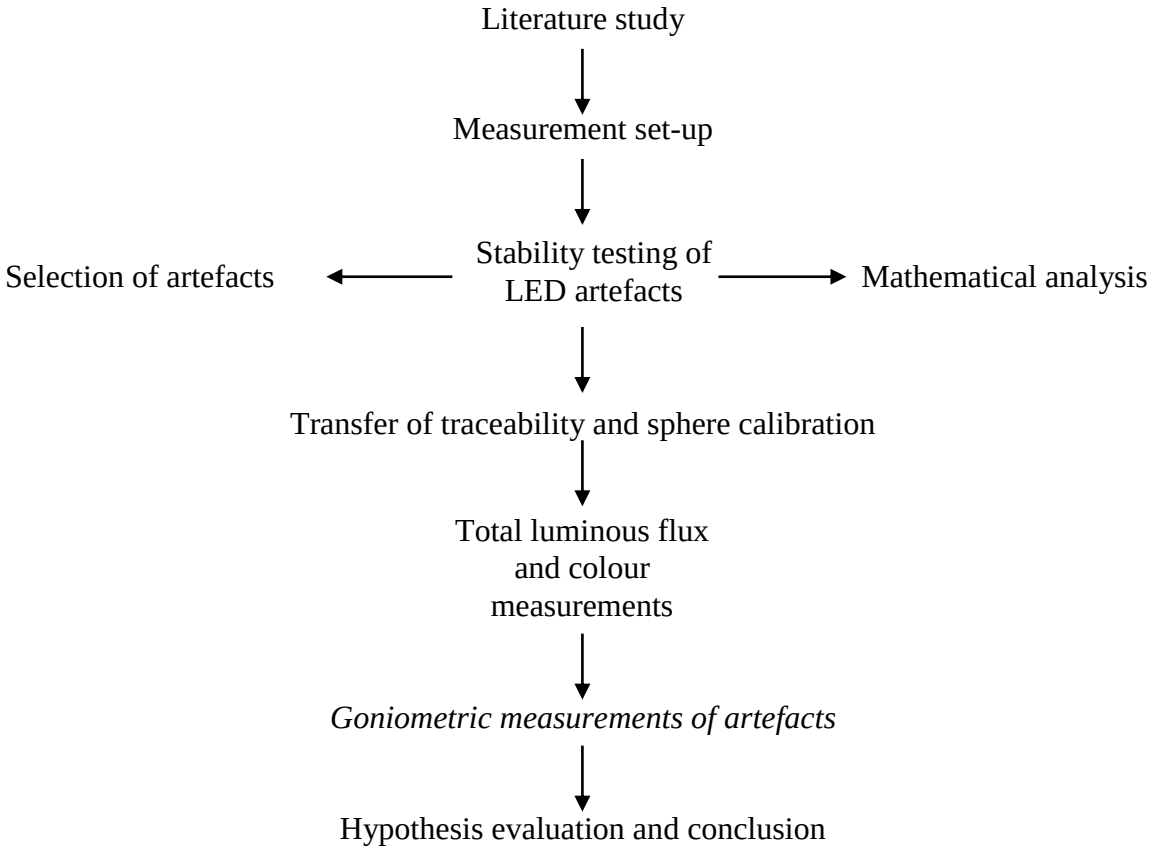

Figure 3.1. Research methodology flow diagram

The hypothesis was tested according to the methodology process illustrated in Figure 3.1. The literature study presented in Chapter 2 was the first task of the process. The fundamental theories, different measurement concepts, measurement instruments used and, most

importantly, the challenges associated with available measurement techniques for LEDs were studied.

In parallel with the literature study, the LED seasoning process and intensity measurements were performed during the selection of LED artefacts designs with acceptable stability and robustness for further measurements. LEDs that maintain stable intensities with ambient temperature kept in the range of 24.5 – 25.5 ^{o}C are assumed to perform the same with total luminous flux measurements inside a sphere.

Upon selection of suitable LED artefacts for colour and luminous flux measurements, a quartz halogen spectral radiant lamp standard (120V 1000W FEL quartz halogen lamp) was prepared for sphere and spectroradiometer calibration. A tungsten filament intensity calibrated lamp (illuminant A standard) was also prepared for flux calibration of the sphere.

Both the total luminous flux and colour measurements were performed using a 76″ sphere set-up at UP, with the measurement method used being that detailed in this research. The spectral measurement method was validated using the method that has been employed by NMISA for decades. This method has undergone a number of international laboratory comparisons, with acceptable standard deviation seen. The proposed luminous flux method can be validated using goniometer measurements by measuring the same artefacts for total luminous flux on a goniometric set-up at UP. However, this is not necessary if the artefacts' correction factors are within the acceptable range.

3.2 SELECTION OF LED ARTEFACTS

The LED artefacts were selected from the rated performances. Although more simply packaged LEDs, like 5 mm epoxy, are easier to measure for its junction voltage whilst taking an optical measurement, the focus was based on packaged LED lamps constructed from high power LEDs. This means that most artefacts in question will have a heat sink, while some even run on alternating current (AC) power supply and have no measuring points for a junction voltage, which is required to monitor and correct for temperature drifting. The criterion was to select the best performing LEDs from two reputable manufacturers. The selection was based on the stability of the output flux and CCT of each LED. A stable CCT is a good sign (but not a ruling condition) of reproducible spectral irradiance measurements

at steady environmental conditions. General lighting lamps were preferable; hence most lamps under study have an E_{27}-base and lumen rating of about 50 – 600 lm.

Figure 3.2. A selection of LED products studied in this research

Figure 3.2 shows a selection of LED products studied in this research. It can be seen that some of the light bulbs have been designed to imitate the shape of incandescent light bulbs.

3.3 PREPARATION AND MEASUREMENT SET-UP

All pre-selected LED lamps were seasoned for 100 hours at respective current or voltage ratings. This is done because some of the new lamps may exhibit flicker or other visual instabilities. This condition might be caused by residual impurities that may be present in a new lamp as a result of normal manufacturing processes or if it is affected by initial phosphor distribution in a new lamp [36]. This is one of the most important tasks to be performed in order to extract different parameters of an LED lamp before measurements are taken. The constancy of parameters such as the heat sink temperature, power supply unit (PSU) current, ambient temperature, and photocell current, were all recorded and monitored. Unlike with advanced LED seasoning methods, like the one presented in [37], none of these parameters were controlled, except for the ambient temperature of the NMISA laboratory, which is air-conditioned and kept in the range of 24.5 – 25.5 ^{o}C.

The equipment and measurement set-up used during the seasoning and selection of LED lamps is shown in Figure 3.3.

(a) (b)

Figure 3.3. (a) Some of the equipment used during the seasoning of LED lamps and b) LED intensity measurement set-up, together with heat-sink temperature monitoring using NMISA calibrated thermistors

The seasoning and intensity measurements were performed on a photometry bench at NMISA. Not too much focus was placed on the uncertainty contributors (such as stray light, alignment and temperature drift correction), as relative measurements would suffice for the selection process.

The equipment used during this first laboratory task is listed in Table 3.1.

Table 3.1. List of equipment used during the seasoning and stability analysis

Item	Manufacturer	Model	Traceability
1) AC source	Yokogawa	MT220	No calibration required
2) Power meter	Yokogawa	2533	No calibration required
3) Digital voltmeter	Agilent	34401a	Calibrated
4) Digital ammeter	Agilent	34401a	Calibrated
5) Photometer head	LMT	S1000	Calibrated

The only critical traceability requirement in this experiment was the calibration certificate of the digital voltmeters (DVM) (which also works as a current ammeter). The AC LED source needed to be powered using a 230 VAC 50Hz power source that is stable in magnitude, frequency and, most importantly, the phase. The change in output intensity of AC powered LED lamps, with respect to input voltage instabilities, was also evaluated. Since the AC source was not calibrated at the time of this experiment, the output power signal

needed to be constantly verified by a DVM. The measurement of heat-sink temperature was also monitored for comparison purposes; the interest was in the change rather than the absolute temperature itself. Nevertheless, the temperature sensors are traceable to the NMISA temperature standard.

The 5 mm epoxy LEDs and other discrete high power LEDs come without driver circuitry for powering and loading the device. Such LEDs were powered according to the manufacturer's recommendations. An inclusion of these LED variants was of utmost importance in this research as, unlike with other driver powered packages, they provide access to the p-n junction for probing junction voltage measurements. LED optical radiation measurement is highly affected by the temperature of the junction T_j, which is proportional to the junction voltage V_j[22 – 25]. When an optical measurement is taken, V_j needs to be recorded for comparison purposes. As the V_j of an LED can be approximated as a linear function of the T_j in a small interval, say ±10 °C, around a reference temperature of T_0, the temperature dependence of its total luminous flux Φ_{LED} can be modelled as a third-order (to keep the correction uncertainties below 0.5%) polynomial with three coefficients:[26]

$$\frac{\Phi_{LED}(T)}{\Phi_{LED}(T_0)} = 1 + a[V_j(T) - V_j(T_0)] + b[V_j(T) - V_j(T_0)]^2 + c[V_j(T) - V_j(T_0)]^3 \qquad (3.1)$$

The coefficients a, b and c of each artefact's LED could be determined by fitting the curve of Equation 3.1 to the functional seasoning data.

3.4 TRANSFER OF TRACEABILITY

Time constraints and the unavailability of usable integrating spheres at NMISA made it necessary to perform some of the measurement experiments at UP lighting laboratories. The experiments performed at the UP laboratories had to be traceable to NMISA's primary standard, i.e. the absolute radiometer. Figure 3.4 shows the traceability of measurements performed from both NMISA and UP to the NMISA's absolute radiometer.

The temperature sensors are traced to NMISA's primary standard for temperature, while the electricity measurements are traced to external reputable calibrating facilities.

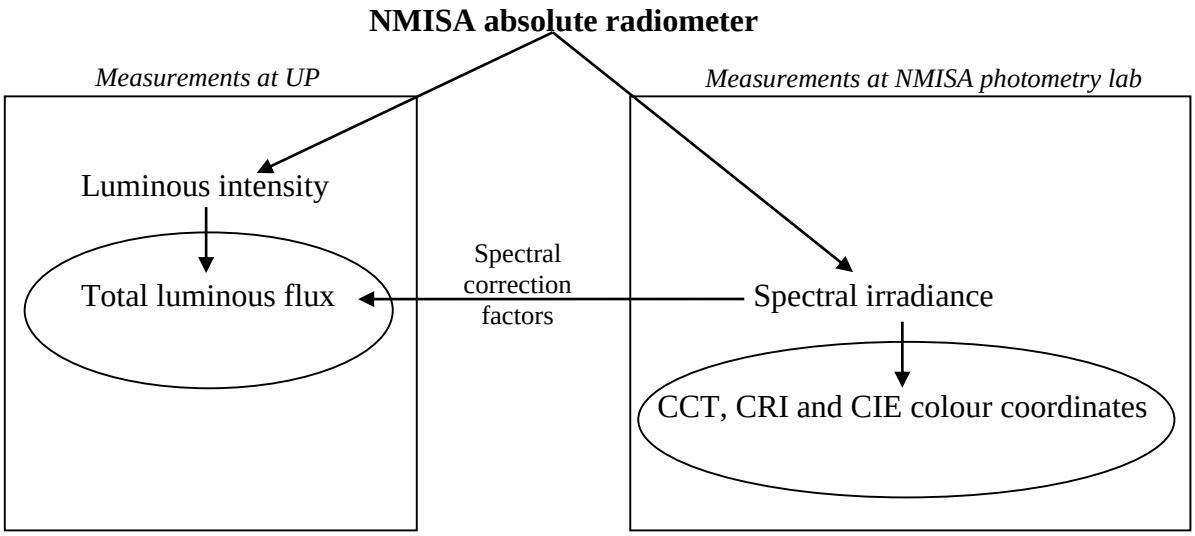

Figure 3.4. Traceability of measurements from both laboratories to NMISA's main primary standard

The spectral measurements of LEDs were performed at UP using a spectroradiometer and a white reflectance standard. The reflectance standard (spectralon tablet) is illuminated with an LED lamp positioned at 45^{o} from the spectroradiometer. Figure 3.5 shows the set-up for the LED colour measurements using a photometry bench at NMISA.

Figure 3.5. LED measurement set-up for colour measurements at NMMISA

The reflectance of the reflectance standard is known, hence the measurement results can be corrected for the errors due to reflectance imperfections.

Before any measurement could be made at the UP laboratory, the traceability from NMISA's giant standard (cryogenic absolute radiometer) had to be transferred. This was done by firstly verifying the spectroradiometer (Konica Minolta CS 2000) used at UP against the Spectra-Scan PR14spectroradiometer, a working standard at NMISA tracing to the primary spectral radiant standard. Both spectroradiometers are shown in Figure 3.6.

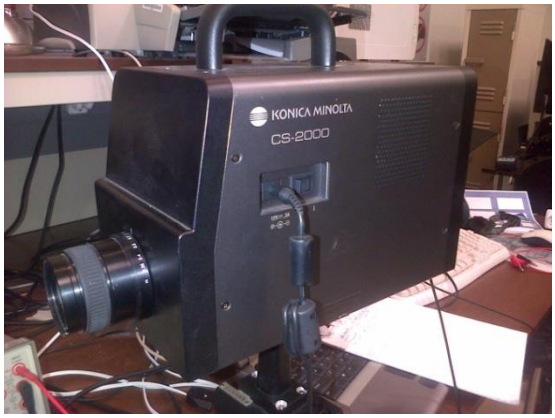

(a)

Figure 3.6.a) The Konica Minolta CS-2000 spectroradiometer used at UP

(b)

Figure 3.6.b) The Spectra-Scan PR14 standard spectroradiometer at NMISA

A quartz halogen spectral radiant lamp standard was recalibrated at NMISA and transported to UP for traceability transfer. This lamp was used to calibrate the CS 2000 spectroradiometer and in turn to calibrate the sphere measurement set-up for relative spectral performance and the relative throughput. Secondly, a lumen was realised from NMISA's illuminance (*E*) standard. External illuminance was then converted to the amount of flux entering the sphere, which was used to calibrate the sensitivity of the sphere. This conversion

of E on a known precision aperture area to φ_i entering a sphere is illustrated in Figure 3.7. A direct comparison method of transferring the luminous flux from the NMISA incandescent standard would have been simpler, but was avoided in order to validate the hypothesis.

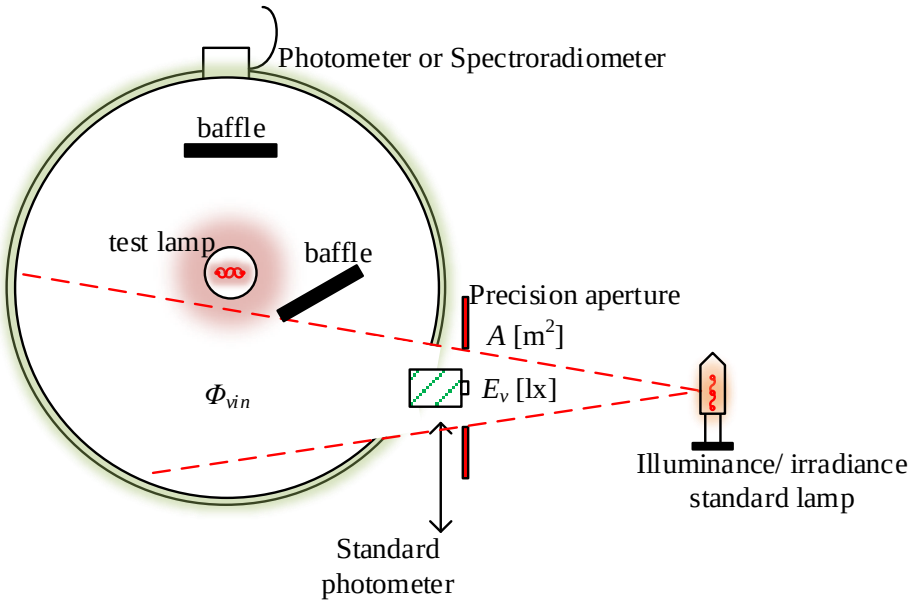

Figure 3.7. The conversion of illuminance to the flux entering the sphere

3.5 MEASUREMENT PROCEDURE FOR LUMINOUS FLUX AND COLOUR MEASUREMENTS

Using a UP 20″ sphere or 76″ sphere, a lumen is realised from an external illuminance standard. The sphere-photometer is calibrated for luminous flux using known input flux into the sphere.

An illuminant A lamp standard used during the transfer of luminous flux was a tungsten filament (blackbody radiator type) lamp, which has very low intensity in lower (blue region) wavelengths. For this reason, a relative spectral throughput of the sphere was determined. Together with the photometer spectral response, these responsivities were used to determine the spectral correction factor of this particular sphere measurement set-up. The following method was followed to measure the total luminous flux of an LED lamp.

The equipment used in this experiment is listed below:

- 20″ spectraflect coated integrating sphere (*integrating sphere with appropriate openings*);

- *Labsphere* current amplifier (*current amplifier to use with a photometer head*);
- *Konica Minolta* CS 2000 spectroradiometer (*a high quality, calibrated CCD arr*ay *spectroradiometer*);
- 100 mm precision aperture (*precision apertures*);
- *LMT* S1000 photometer head (*a high quality photometer head traceable to an NMI illuminance and spectral responsivity standard*);
- Distance measuring tape (*a photometric bench with calibrated distance measure is desired*);
- 1000 W quartz halogen spectral radiant lamp (*a spectral radiant standard lamp*);
- 75 W luminous intensity lamp (*illuminant A standard lamp*);
- *Goldilux* illuminance meter (*a calibrated photometer head/illuminance E meter*);
- 1000W current stable power supply unit (*PSU*); and
- Calibrated digital multimeter (*DVM and DMM*).

The following is a step-by-step method for measuring the total luminous flux of LEDs using a modified absolute luminous flux measurement.

1. Preparation of measurement equipment:
    1.1. The measurement equipment, test lamps and standard meters must be stored inside the measurement laboratory to allow for acclimatisation in the laboratory conditions, for 24 hours. The recommended laboratory temperature is 24 ± 2°C [28].
    1.2. The lamps (standard and test) should be kept clean or wiped of finger prints and dirt using an appropriate cloth supplied by the manufacturer.
2. Alignment for spectral characterisation of the sphere set-up:
    2.1. A spectroradiometer is aligned at 45° angle with a white reflectance standard (with known traceable reflectance) and a spectral radiant standard, as shown in Figure 3.8 below. A calibrated distance *d* between the lamp and a reflectance standard is the same distance a standard lamp was calibrated from the measuring detector. It is usually stated on the calibration certificate.

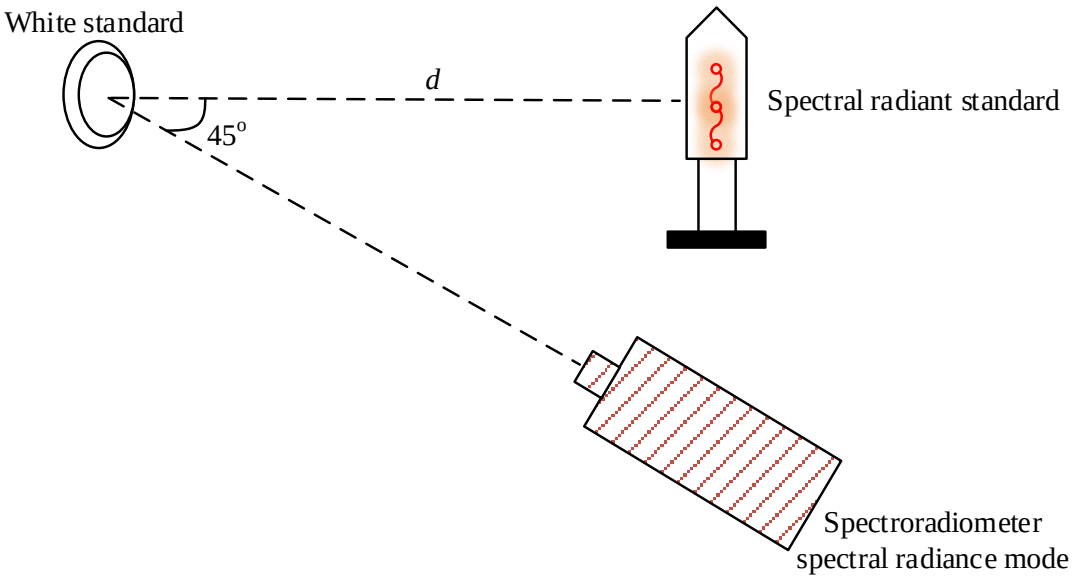

Figure 3.8. The set-up used for spectral irradiance measurements

2.2. The measured spectral radiance is converted to spectral irradiance using the reflectance of the white reflectance standard and compared with the spectral irradiance of the standard lamp. If desired, correction factors can be noted in order to make all the spectral measurements traceable to the spectral radiant standard from this point onwards.

2.3. The set-up in Figure 3.9 is used to measure the throughput of the integrating sphere set-up.

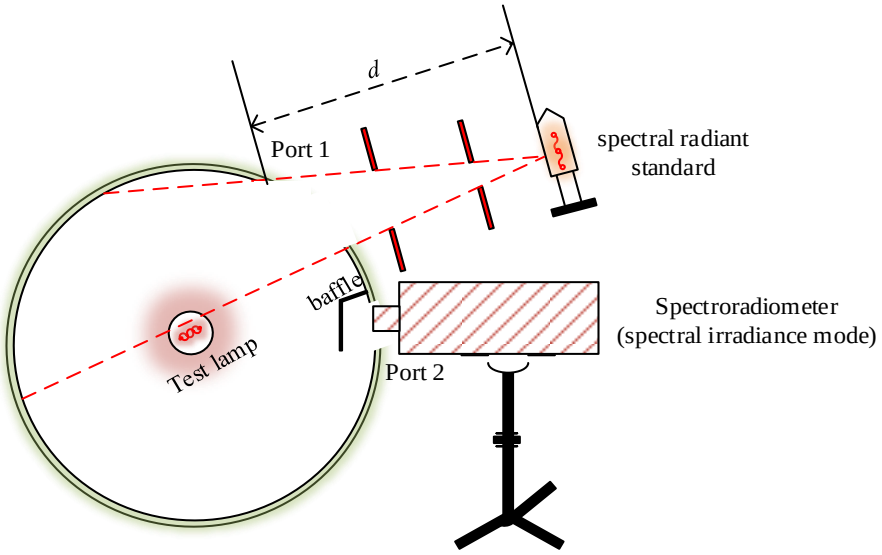

Figure 3.9. The set-up used to measure the throughput of the integrating sphere set-up

2.4. A known spectral irradiance is introduced into the sphere and measured using a spectroradiometer. The throughput $R_s(\lambda)$ is obtained from Equation 3.2 below, where s_{out} and s_{in} represent the spectral irradiance outside the sphere opening and inside the sphere, respectively:

$$R_s(\lambda) = \frac{s_{out}(\lambda)}{s_{in}(\lambda)} \tag{3.2}$$

2.5. Port 1 can now be closed and a UUT(unit under test) can be lit for more than 20 minutes and measured for spectral irradiance. The normalised spectral irradiance measured can be treated as $s_{LED}(\lambda)$.

2.6. The spectral irradiance of illuminant A intensity standard can be measured using a set-up as shown in Figure 3.9 and normalised in order to have $s_{cal}(\lambda)$.

$$F = \frac{\int s_{LED}(\lambda)V(\lambda)d\lambda . \int s_{cal}(\lambda)s_{rel}(\lambda)d\lambda}{\int s_{LED}(\lambda)s_{rel}(\lambda)d\lambda . \int s_{cal}(\lambda)V(\lambda)d\lambda} \tag{3.3}$$

The characterisation of an integrating sphere from 2.1 to 2.6 can be done only once in a while, except for step 2.5 for the measurement of the UUT spectrum, which is an unknown variable for every UUT. The objective of the above measurements is to calculate for spectral mismatch correction factor *F*, which is then used as a multiplier for the results obtained in step 3 below.

3. Alignment for luminous flux characterisation of the sphere-photometer set-up:
The purpose of this step is to introduce a known luminous flux (measured externally with a traceable illuminance meter) into the integrating sphere and measure it with a sphere photometer head.

3.1. A sphere aperture of size d_0 is used to introduce flux from a calibrated illuminant A lamp standard into the integrating sphere. A standard illuminance meter is used to measure the illuminance at this position.

3.2. The photometer head (photodiode) is expected to give a linear sensitivity curve over a wide range of flux introduced into the sphere. The current amplifier is zeroed at darkness, when there is no light detected by the photometer head.

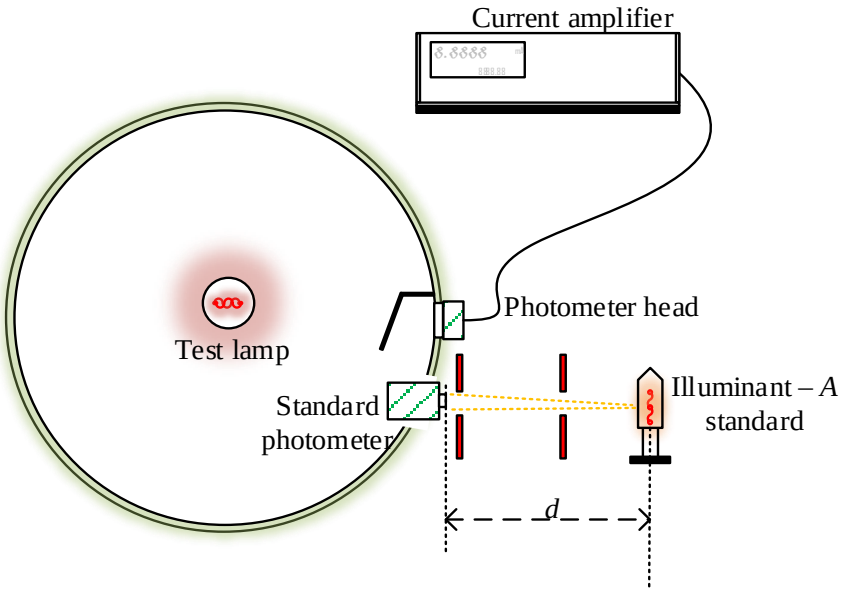

Figure 3.10. The set-up used to calibrate the integrating sphere for intensity measurements (lumen realisation)

3.3. Measurements at five or more various distances between the illuminance meter and the illuminant A standard lamp can be chosen while the lamp current and alignment is carefully kept constant.

3.4. For each of the positions, illuminance is measured at the entrance of the aperture, and then illuminance meter is removed to allow the same flux to enter the sphere. Finally a current measurement is taken on the photodiode current amplifier.

3.5. The measured illuminance is translated to input flux using the Equation below:

$$E_{aper} = \frac{\Phi_{in}}{A_{aper}} \tag{3.4}$$

where A_{aper} is the aperture/opening area and E_{aper} is the measured illuminance.

3.6. A sensitivity curve representing the whole sphere-photometer set-up can be calculated using the measurement data above. The sensitivity curve of a photodiode is assumed to follow a straight line curve:

$$\Phi_{LED} = mI_{photodiode} + c \tag{3.5}$$

Parameters ***m*** and ***c*** are calculated from the measurement data in the previous steps. They characterise a measurement set-up. Recalibration of these parameters will be necessary if any of the equipment or its calibration values changes.

3.7. The illuminance meter aperture is then closed and the UUT lit for 20 minutes before a measurement can be taken.

3.8. The measured luminous flux can then be corrected by multipliying the results with a spectral mismatch factor *F* calculated in step 2.6.

CHAPTER 4 MEASUREMENT RESULTS

4.1 INTRODUCTION

Chapter 4 is dedicated to a discussion of how the total luminous flux and spectral measurements were approached. The chapter deals with the application of measurement methodologies discussed in Chapter 3. The methods are tested and validated by goniometric measurements. The actual measurements for luminous flux are performed using a 2m sphere at UP. The measurements for transferring traceability from the following NMISA standards are also discussed:

- Spectral radiant standard – irradiance parameter is observed as a function of wavelength λ. This provides traceability for the Konica Minolta CS 2000 spectroradiometer from the Photo Research SpectraScan PR-714 spectroradiometer (NMISA standard).
- White reflectance standard – while both the spectroradiometers are operated in radiance mode, a known white reflectance standard is used to measure spectral radiance, which is then converted into spectral irradiance.
- Intensity standard – a NMISA standard illuminance meter is borrowed by UP, for the calibration of flux entering the sphere. This meter is calibrated using an illuminant A type lamp standard, while a 75W tungsten-filament lamp is used for the set-up at UP.

All three standards above were necessary to provide traceability between the UP laboratory and NMISA.

4.2 SPECTRAL IRRADIANCE TRANSFER

A spectral radiant standard lamp from NMISA was used to verify the Konica Minolta CS 2000 that was used at the UP laboratory for these experiments. A spectroradiometer was focused on a white reflectance standard of known spectral responsivity over the visible spectrum. A spectral radiance was measured on a white standard, and converted to spectral irradiance using the spectral responsivity of the white standard.

4.3 LUMINOUS FLUX TRANSFER

A *Goldilux* calibrated working standard illuminance meter with a cosine corrected probe was used to transfer illuminance traceability from NMISA to the UP laboratories. This illuminance was calibrated using an illuminant A working standard lamp at NMISA. It was also adjusted to give corrected illuminance values. Since an illuminant A (same CCT value as the lamp used to calibrate this meter) standard lamp was used at UP to introduce flux inside the sphere, no spectral mismatch correction is required on the values read from the meter. A *Goldilux* illuminance meter with a cosine corrected probe is shown in Figure 4.1.

Figure 4.1. A cosine corrected probe of an illuminance meter by *Goldilux*

The luminous flux realisation presented in this work traces directly from the intensity (candela) standard of NMISA. It should also be noted that a meter is used as a working standard, as opposed to traditional measurement set-ups where a lamp is used as a tracing standard.

4.4 RELATIVE SPECTRAL RESPONSIVITY OF SPHERE

The spectral responsivity of the sphere is directly related to, but is not, the spectral reflectance of the coating used, which is $BaSO_4$ (spectraflect coating by *Labsphere*) in this case.

The spectral responsivity of the integrating sphere or the throughput is the ratio between the output and the input spectral power density (SPD) of a spectral flux introduced into the integrating sphere. A simple way to measure this is to take a known spectral radiant flux standard (usually a quartz halogen lamp would be used) and set up a 4π measurement inside a sphere. The spectroradiometer measures the output flux over the entire wavelength of interest.

One of the limitations of this project was the unavailability of all the necessary equipment. A portable spectroradiometer was used instead of a sphere-spectroradiometer, as depicted in Figure 4.2a. Only a bench spectral radiant flux lamp standard (calibrated on its upside down position) was available at the time when the measurements were performed, depicted in Figure 4.2b.

Figure 4.2. (a) A portable spectroradiometer used at UP

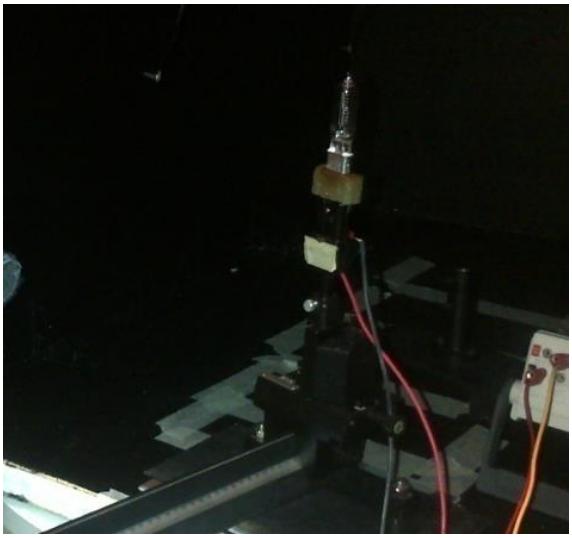

Figure 4.2. (b) A bench spectral radiant flux standard lamp (a 120V 1000W FEL quartz halogen lamp by *Osram Sylvania*)

For this project, the spectral irradiance flux was measured on a bench at the same position the spectral radiant standard was calibrated; this is just for verification purposes. The spectral irradiance flux entering the sphere is known. A portable spectroradiometer is configured in irradiance mode and placed on the same port where the *LMT* photometer is placed to measure the luminous flux inside the sphere. The measurement set-up is shown by the picture in Figure 4.3.

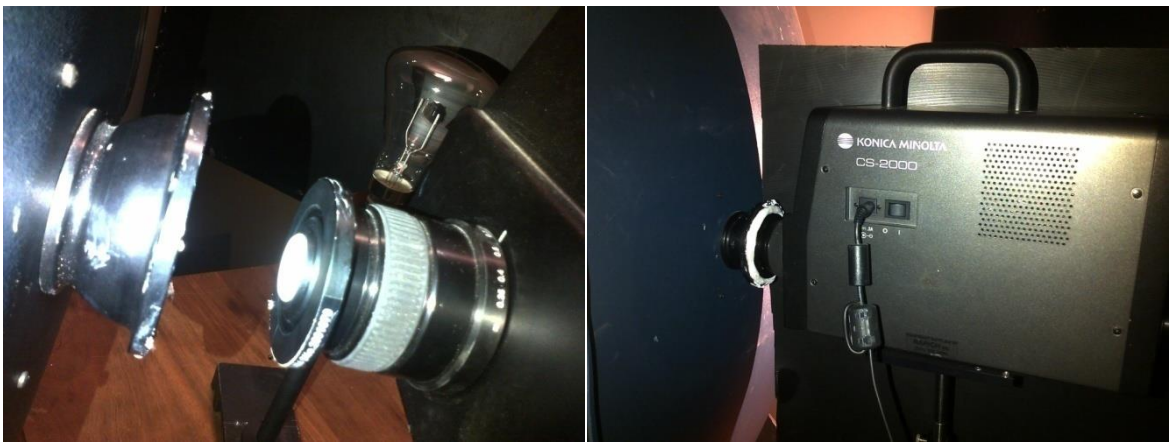

Figure 4.3. Measuring the relative spectral responsivity of the integrating sphere

Since we are only interested in the spectral performance of the throughput, both the input flux and the output measured were normalised to one before the ratio was calculated. The throughput of the 76 integrating sphere is shown in Figure 4.4.

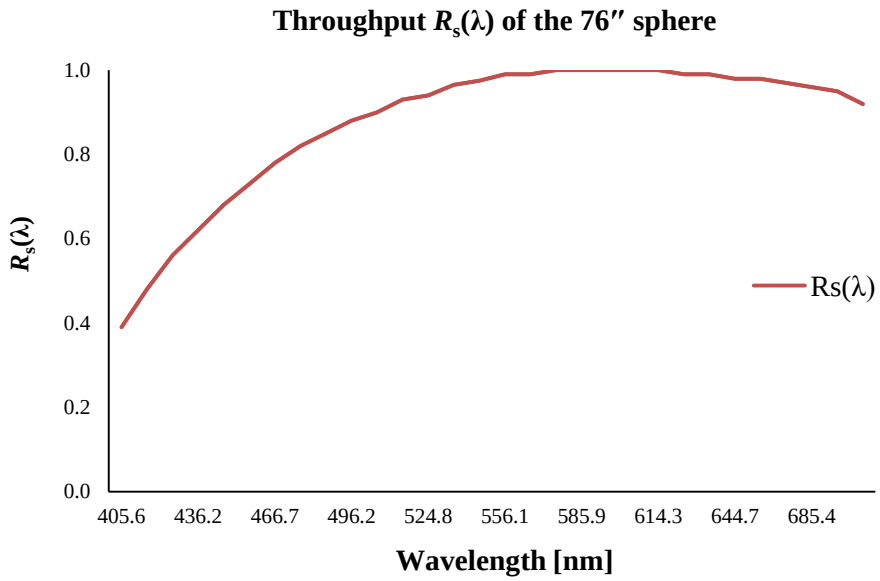

Figure 4.4. The measured throughput of a 76″ integrating sphere by *Labsphere*

It can be noted that the throughput of the sphere is not as flat as the reflection curve of a flat spectraflect coated block, especially around shorter wavelength region.

4.5 MEASURING LINEARITY OF THE PHOTODIODE AND SPHERE CHARACTERISATION

The sphere was calibrated using an illuminant A lamp from NMISA (see Figure 4.5).

Figure 4.5. A tungsten filament illuminant A lamp from *NMISA*

This lamp gives enough flux inside the sphere, at different selected distances; thus the linearity of the sphere-photodiode set-up can be measured.

Figure 4.6. Set-up for calibration of the sphere sensitivity

A 76″ sphere is used (bigger sphere – worst case) to prove that the methodology works for an acceptable sphere size range. The sphere has a 12cm diameter opening on the side. Flux is measured using a calibrated working standard *Goldilux* illuminance meter. Seven different

positions away from the aperture are measured and marked (distance calibration is not important as only illuminance at the sphere opening is considered). At each distance, a lamp is positioned such that the illuminance meter measures uniformly throughout the aperture opening. A $V(\lambda)$ filtered photodiode with f_1' (measure of goodness of fit between the detector filter to a theoretical V(λ)) of 4% is used with a state-of-the-art *Labsphere* photocurrent amplifier (able to detect light current from pico-amps range). This calibration is done with the UUT inside a sphere, with the UUT switched off.

Table 4.1. Calibration data for a 76″ sphere flux measurements

Position [cm]	Illuminance [lux]	Photoelement current [nA]	Flux [lm]
120	192.0	42.40	0.965
100	233.7	52.63	1.175
80	293.0	66.65	1.473
60	373.5	85.35	1.877
50	446.5	102.00	2.244
40	618.5	141.85	3.109
30	2775	614.70	13.949

Table 4.1 shows the results of flux introduced into the sphere at seven different distances while measuring the illuminance for each distance. A fitted curve of Table 4.1 results is then depicted in Figure 4.8.

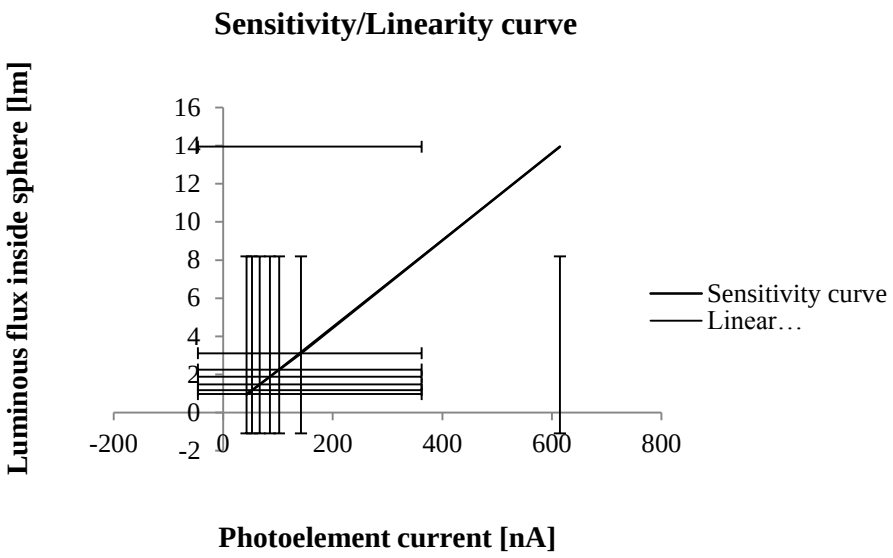

Figure 4.7. Linearity curve for sphere-photo diode set-up

As expected, a silicon photo diode should have a linear responsivity as shown in Figure 4.7 with a linear curve calculated to give Equation 4.1. Equation 4.1 is taken as a unique equation that is considered a characterisation of the specific integrating sphere-photometer set-up used at the University of Pretoria lighting laboratory (used for all the measurements in this thesis).

Following the above linear curve:

$$\Phi_{LED} = 0.02168 I_{photodiode} + 0.03350 \qquad (4.1)$$

A 4000K *Pharox* 400 lm rated white LED lamp reads the photodiode current of 18835 x 10^{-9}A current after stabilising for 30 minutes, as shown in Figure 4.8.

Figure 4.8. A *Pharox* 400 lm rated white LED lamp allowed to stabilise for 30 minutes inside an opened sphere before photo-diode measurement is taken

Substituting the value of this current reading in Equation 4.1 gives a total luminous flux of 408.38 lm for this LED lamp. It must be noted that this is the value before the spectral correction has been applied for this lamp. The calibration was done using illuminant A lamp (very low blue content). Taking also the f_1' of photometer into account, we expect the correction factor of a phosphor-based and blue coloured LED to be greater than unity, depending on its bandwidth and blue content.

4.6 MEASUREMENT RESULTS FOR SELECTED LED ARTEFACTS

LED artefacts that proved to be stable during the seasoning process were selected for hypothesis verification of this study.

4.6.1 Luminous flux measurements

Table 4.2 shows the total luminous flux measured for 6 selected lamps. Despite the stability characteristics of selected LEDs, they were also selected according to differing colour temperatures, lumen levels and types. For verification purposes, 2 incandescent lamps were added on the list to verify the method even further.

Table 4.2. Measurement results for 6 selected artefacts

Lamp measured	Lamp type	Labelled luminous flux [lm]	Photodiode current after stabilisation [nA]	Total luminous flux measured [lm]
Pharox 400 lm 2800 K	LED	400	18835	408.38
Philips 150 lm 4000 K	LED	150	7075	153.42
Kwalico 350 lm 4000 K	LED	350	16882	366.04
Osram 100W bulb ~2800 K	Incandescent	900	42652	924.73
Osram 60W bulb ~2800 K	Incandescent	400	19102	414.16
Pharox 4000 K	3-LED (RGB) model	150	7114	154.27

The measured total luminous flux for each lamp is presented and does not deviate much from the expected value as labelled by each lamp manufacturer.

4.6.2 Spectral correction of measured luminous flux

Using the calibration certificate provided by *LMT* for the photometer head, its response is plotted annotated with a CIE $V(\lambda)$ curve in Figure 4.10. f_1' is calculated to be 1.13% using Equation 2.16, compared to the specified 1.3% on the calibration certificate.

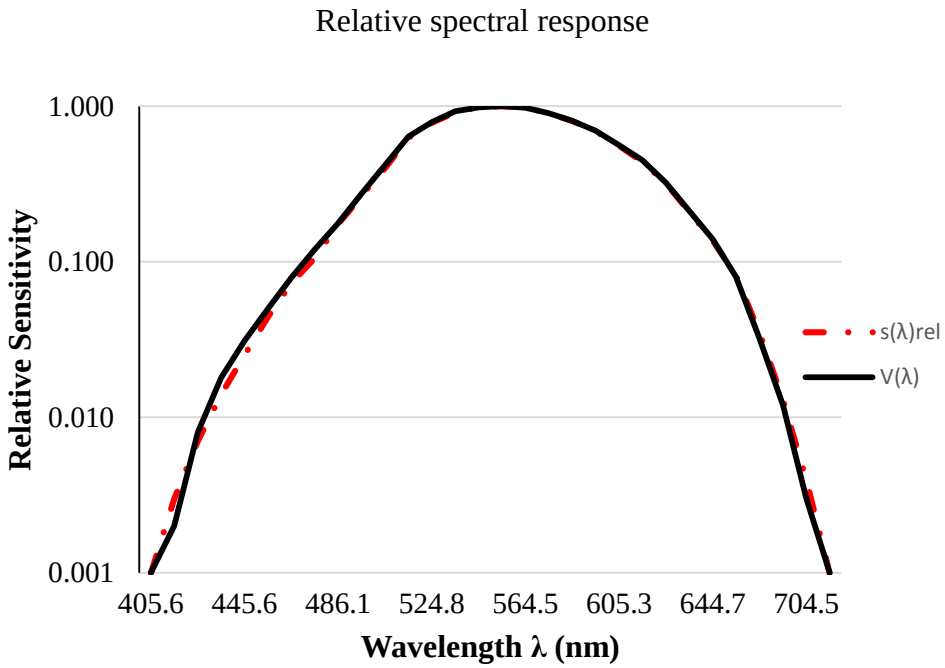

Figure 4.9. The performance of the *LMT* S1000 photometer head against a *V*(λ) curve

Figure 4.10 shows the relative error of the *LMT* S1000 meter head used in the experiments. It can be noted that a low f'_1 is not good enough in the case of monochromatic sources like the LEDs. A correction still needs to be applied in order to minimise errors.

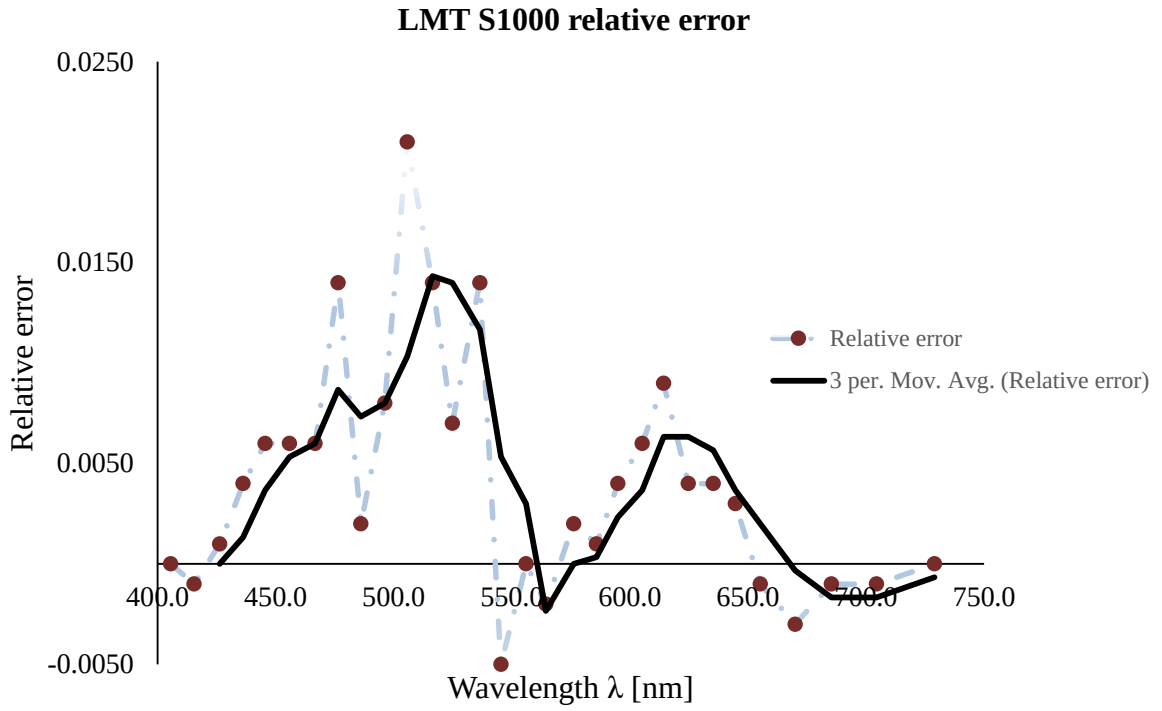

Figure 4.10. The relative error of the LMT S1000 meter head

The correction factor used to correct the luminous flux measurements discussed in section 4.6.1 is given by:

$$F = \frac{\int s_{LED}(\lambda)V(\lambda)d\lambda . \int s_{cal}(\lambda)s_{rel}(\lambda)d\lambda}{\int s_{LED}(\lambda)s_{rel}(\lambda)d\lambda . \int s_{cal}(\lambda)V(\lambda)d\lambda} \quad (4.2)$$

where

$s_{LED}(\lambda)$ is the spectral power distribution (SPD) of the UUT;

$s_{cal}(\lambda)$ is the SPD of the illuminant A standard source; and

$S_{rel}(\lambda)$ is the relative spectral responsivity of the sphere system.

The SPD $s_{LED}(\lambda)$ of an LED can be accurately measured using a spectroradiometer and normalised to one for the purpose of this calculation. The SPD (spectral power distribution) of the illuminant A can also be measured and verified with a calibration certificate. A challenge is to characterise the responsivity of the whole measuring system $S_{rel}(\lambda)$. The

uncertainties of the measurement will be very dependent on how good this parameter can be characterised for each measurement system. This spectral responsivity includes the response of the integrating sphere, measuring meter, opal glass (when it is used, and which is not used in this experiment) and mismatches brought by the spectroradiometer. In a closed measurement system, a dedicated software application would attempt calibrating the entire sphere system before taking a measurement.

The normalised SPD of the illuminant A lamp and UUT can be read from a calibration certificate and measured using a spectroradiometer, respectively. Both SPDs were measured in this experiment to verify the given calibration data of the illuminant A lamp. The throughput component is very important as it characterises a particular integrating sphere. A lengthy discussion on integrating sphere throughput has been presented in section 4.4 and results are shown in Figure 4.4 for this particular integrating sphere used in this experiment. All components needed in the calculation of a spectral correction factor *F* have been shown in Figure 4.12. This is for a 4000 K Pharox 400 lm LED lamp.

Figure 4.11. A 4000K CCT white LED lamp total luminous flux measurement

It should be noted that none of the spectral measurements in this experiment were taken using an integrating sphere. A spectralon white standard was used instead in order to prevent accounting for integrating sphere impurities that are being corrected for in this study.

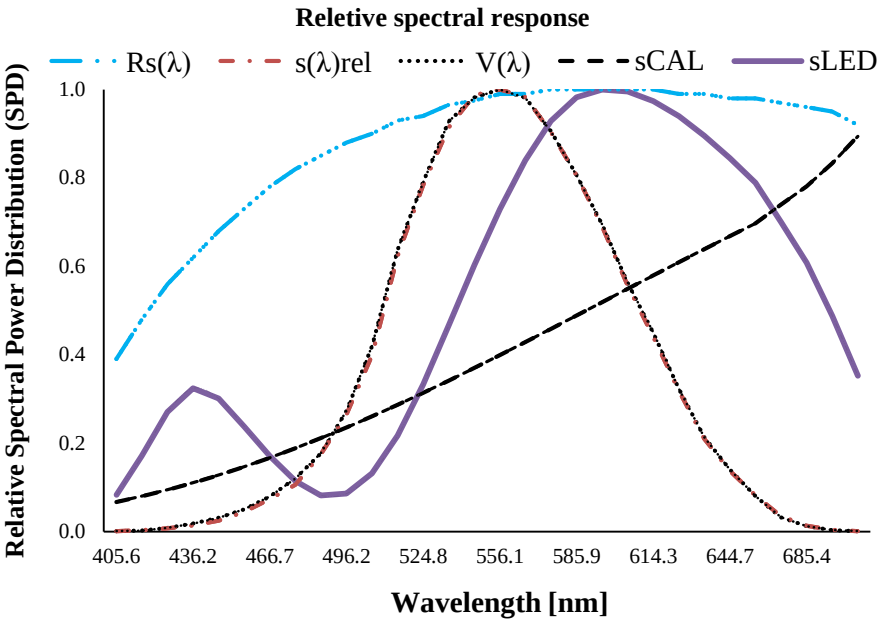

Figure 4.12. Spectral components used to calculate spectral correction factor *F*

Making use of the *F* factor equation, an Excel spread sheet was created for this experiment. Since for every measurement the total luminous flux of all the SPDs required for the equation will be known, only the SPD of the UUT needs to be measured and used as an input parameter to the equation.

Table 4.3. Measurement results for 6 selected artefacts

Lamp measured	Lamp type	Labelled luminous flux [lm]	Total luminous flux measured [lm]	Correction factor *F*	Spectrally corrected luminous flux [lm]	% corrected error
Pharox 400 lm 2800 K	LED	400	408.38	1.0004	408.54	0.04
Philips 150 lm 4000 K	LED	150	153.42	1.0039	154.02	0.40
Kwalico 350 lm 4000 K	LED	350	366.04	1.0023	366.88	0.23
Osram 100W ~2800 K	Incandescent	900	924.73	0.999942	924.68	0.005
Osram 60W ~2800 K	Incandescent	400	414.16	0.999921	414.13	0.007
Pharox 4000 K	3-LED (RGB) model	150	154.27	1.00652	155.28	0.66

The calculated spectral correction factors for each lamp are presented in Table 4.3 together with their corrected errors.

4.7 CONCLUSION

Surprisingly, even the worst spectral corrected errors of the selected lamps would be disregarded for a measurement facility that does not have stringent requirements on measurement uncertainties and accuracies.

CHAPTER 5 DISCUSSION

5.1 TRACEABILITY

The integrity of the results presented in the previous chapter relies on the traceability with a reputable national laboratory. The methodology formulated in this study bases its traceability from 3 standards, namely: the spectral radiant standard (spectroradiometer verification and all spectral measurements thereafter), the white reflectance standard (all spectral irradiance measurements except for the sphere throughput are measured in radiance mode) and the intensity standard (for the realisation of a lumen from a candela).

5.2 LOW LUMEN ILLUMINANT A CALIBRATION LAMP

Although very low lumen levels were introduced into the integrating sphere, larger sized spheres also play a negative role (expected to have a comparably lower throughput), the S1000 photometer head tolerated low levels of light and performed exceptionally well in terms of linearity. The tungsten filament illuminant A lamp only managed around a lumen of up to 14 lm entering an integrating sphere over the selected distances during the lumen calibration/realisation of the integrating sphere. This pioneer set-up is still able to measure lumen levels in the region of 1000 lm with acceptable correction factors. High correction factors means very poor measurement uncertainty (MU), i.e. low confident levels, which necessitate the verification of these kinds of measurements with another method.

5.3 HOMOGENEITY AND SPHERE RECALIBRATION

The presented throughput $R_s(\lambda)$ combines the effect of baffles inside the sphere, coating defects and the homogeneity of the sphere. It is a very sensitive parameter that needs to be verified after a certain period of time to account for ageing, dirt inside the sphere and even the slight change of baffle arrangements inside the sphere. Thanks to the high-end photometer head with a good cosine correction, the poor integration capability of a 50cm (smaller) sphere did not show any noticeable change on the performance of the photometer head used.

5.4 PERFOMANCE OF THIS METHOD FOR MEASUREMENT OF OTHER LAMP TYPES

It is expected that blackbody radiator lamp types will have a correction factor value *F* approaching unity for this method. This is due to the fact that this method is tracing to an illuminance meter that is calibrated using another black-body type lamp (tungsten filament). This is also a reason why the lux values entering the sphere read by the illuminance meter did not have to be spectrally corrected. Phosphor-based white LEDs usually have a sharp blue peak. The calibrating lamp (illuminant A) has a very low content on the blue wavelength band, hence the measured value is usually underestimated (therefore correction factors are larger than unity). Unless very low uncertainties are desired, monochromatic LED sources do not have to be measured for SPD all the time in order to characterise the correction factor *F*. For example, an average red LED SPD can be used in the calculation in the case where a monochromatic red LED UUT is measured.

CHAPTER 6 CONCLUSION

In this dissertation, a new AISM is presented and tested using selected LED artefacts. In this method, an integrating sphere is characterised using equipment that can be available in any photometry laboratory, namely: an integrating sphere with at least two windows, illuminance meter (calibrated with an illuminant A standard lamp), a photometer (preferably with a good sensitivity – Nano-amperes range), calibrated quartz halogen lamp and a tungsten filament lamp. For day-to-day measurements of LED lamps of known SPD, only an integrating sphere and a photometer are used to perform a measurement. The minimum lumen levels characterised for in this study were as small as 1lm; this could be even smaller with the reduction of the sphere diameter. The maximum lumen levels that can be successfully measured can be as high as the photodiode is able to take.

This method eliminates the need for standard LEDs, which need to resemble the UUT in many aspects (lumen levels, SPD and spatial density). Having a standard LED for each and every UUT would come with some financial implications. Standard lamps are expensive, require sophisticated storage and they age. The method presented enjoys the benefits of tracing from a meter standard as opposed to a lamp standard. This is by far a huge improvement from the lamp standard reference measurement for total luminous flux.

The measurements performed on the selected lamps compare very well with the claimed lumen values by the manufacturers. Depending on a particular UUT's SPD and desired accuracies, it may not even be necessary to apply the spectral correction if the photometer head being used has a good f'_1 value (goodness of fit to a $V(\lambda)$ curve), say less than 2%.

6.1 RECOMMENDATIONS FOR FUTURE WORK

- It is recommended that a tried and tested method be used to validate a new methodology. This is usually done through a bilateral comparison where two laboratories agree on the same measurement conditions (room temperature, humidity

and electrical power set-up), measure the same artefacts and compare the results. Due to time constraints and financial implications, this was not viable for this project.

- An available photometer head was used for this study, and was the only option due to its high quality and scarcity. The wavelength increments of the measured responsivity do not match those of a spectroradiometer used. This means that some data points had to be curve fitted. This is not such a good practise in photometry as some data points are not real measured values but assumed values based on available data. Due to time and financial constraints, responsivity verification could not be done for the photometer head.
- It is always a recommended practise and a norm to perform measurements of this nature on a distance calibrated photometry bench. The UP photometry laboratory is not equipped with such equipment. Although measurements performed for this study were adequate for validating the hypothesis, measurement uncertainties should be included with reasonable confident levels.
- The hypothesis validation can be improved further by the inclusion of monochromatic LEDs in this study, which are expected to perform poorly when it comes to spectral error corrections.

REFERENCES

[1] C. C. Miller and Y. Ohno, "Luminous Flux Calibration of LEDs at NIST," in *Proceedings of the 2nd CIE Expert Symposium 2001 on LED Measurement - Standard Methods for Specifying and Measuring LED and LED Cluster Characteristics*, 11 – 12 May, 2001, Gaithersburg, Maryland (USA).

[2] J. Hovila, P. Toivanen and E. Ikonen, "Realization of the Unit of Luminous Flux at the HUT Using the Absolute Integrating-Sphere Method," *Metrologia*, vol. 41, pp. 407–413, November 2004.

[3] Commission Internationale de l´Éclairage. (1997). CIE (1997) Measurement of LEDs: CIE Publication No. 127. CIE. Vienna, Austria, [Online]. Available: http://www.cie.co.at/index.php/index.php?i_ca_id=402.

[4] D. Di Laura et al. (2011). The Lighting Handbook, 10th Ed. Illuminating Engineering Society (IES). Savannah, USA. [Online], Available: https://www.ies.org/handbook/.

[5] Instrument Systems GmbH. (1998). Handbook of LED Metrology, ver. 1.1. Instrument Systems. Munich, Germany. [Online]. Available: http://www.instrumentsystems.com/applications/led-test-measurement/.

[6] P. Maaskant, M. Akhter, and L. Considine, "Failure Mechanisms Associated with the Fabrication of InGaN Based LEDs," *IEEE Trans. On Electron Devices*, vol. 48, no. 8, pp. 1822–1825, August 2001.

[7] M. Arik, J. Petroski, and S. Weaver, "Thermal Challenges in the Future Generation Solid-State Lighting Applications: Light Emitting Diodes," in *Proceedings of the ASME/IEEE ITHERM Conference*, 1–1 June, 2002, San Diego, USA.

[8] F. Yin, W. Guo, T. Ding, W. Yan, and D. Cui, "Thermal and Optical Properties of Power LEDs," in *Proceedings of the Advances in Optoelectronics and Micro/Nano-Optics (AOM), 2010 OSA-IEEE-COS Conference*, 3–6 December, 2010, Guangdong, China.

[9] A. Mills, "Lighting: The Progress and Promise of LEDs," *III-Vs Review*, vol. 17, no. 4, pp. 39–41, May 2004.

[10] E. Hong, "A Non-contact Method to Determine Junction Temperature of High-Brightness (AlGaInP) Light-Emitting Diodes," Master's thesis, Rensselaer Polytechnic Institute, 2003.

[11] Y. Ohno, "Detector–Based Luminous Flux Calibration Using Absolute Integrating Sphere Method," *Metrologia*, vol. 35, no. 4, pp. 473–478, 1998.

[12] Y. Ohno, "New Method for Realizing a Total Luminous Flux Scale Using an Integrating Sphere with an External Source," *J. IES*, vol. 24, no.1, pp. 106–115, 1995.

[13] C. C. Miller, Y. Zong, and Y. Ohno, "LED Photometric Calibrations at the National Institute of Standards and Technology and Future Measurement Needs of LEDs," in *Proceedings of the SPIE* 5530, *Fourth International Conference on Solid State Lighting*,2004 © SPIE. doi:10.1117/12.566635.

[14] Labsphere. (2003). A Technical guide to Integrating Sphere Radiometry and Photometry. Labsphere. North Sutton, USA. [Online]. Available: https://www.labsphere.com/technical-library/

[15] Labsphere. (2003). The Radiometry of Light–Emitting Diodes – LEDs. Labsphere. North Sutton, USA. [Online]. Available: https://www.labsphere.com/technical-library/.

[16] Y.W. Kim, D.H. Lee, S.N. Park, M.Y. Jeon, and S. Park, "Realization and Validation of the Detector-based Absolute Integrating Sphere Method for Luminous-flux Measurement at KRISS," *Metrologia*, vol. 49, no. 3, March 2012.

[17] Lumileds Holdings B.V. (2015, May). Optical Measurement Guidelines for High-Power LEDs and Solid State Lighting Products (White paper). Lumileds. Aachen, Germany. [Online]. Available: http://www.lumileds.com/.

[18] Illumination Engineering Society (IES). (2008). Approved Method: Electrical and Photometric Measurements of Solid-State Lighting Products: Publication LM-79-08.

IES. New York, USA. [Online]. Available: https://www.ies.org/store/product/approved-method-electrical-and-photometric-measurements-of-solidstate-lighting-products-1095.cfm

[19] D. Kasper, "National LED Performance Standard Highlighting Relative Absolute Photometry, presented at the ninth annual IESSA Conference and Annual General Meeting, 2013, Johannesburg, RSA.

[20] A. Höpe, "Diffuse Reflectance and Transmittance," in *Spectrophotometry: Accurate Measurement of Optical Properties of Materials (Experimental Methods in the Physical Sciences)*, 1st Ed., vol. 46,T.A. Germer, J.C. Zwinkels, and B.K. Tsai, Eds.,Walthan, USA: Academic Press, 2014.

[21] T. Poikonen, "Characterization of Light Emitting Diodes and Photometer Quality Factors", Doctoral dissertation, Aalto University, 2012.

[22] Commission Internationale de l´Éclairage. (1987).Methods of Characterizing Illuminance Meters and Luminance Meters: CIE Publication No. 69. CIE. Vienna, Austria. [Online]. Available: http://www.cie.co.at/index.php?i_ca_id=921

[23] Y. Ohno, "A Numerical Method for Color Uncertainty," in *Proceedings for the CIE Expert Symposium on Uncertainty Evaluation*, Vienna, Italy, 2001, pp. 8 – 11.

[24] E. Ikonen, T. Poikonen, P. Kärhä, P. Manninen, and F. Manoocheri,"Determination of f_1' and its Uncertainty with Biased and Random Error Models," in *Proceedings of the CIE Expert Symposium on Advances in Photometry and Colorimetry*, Turin, Italy, 2008, pp. 55–58.

[25] S. Winter and A. Sperling, "Uncertainty Analysis of a Photometer Calibration at the DSR Setup of the PTB," in *Proceedings of the 2nd CIE Expert Symposium on Measurement Uncertainty*, Braunschweig, Germany, 2006, pp. 139–142.

[26] U. Krüger and G. Sauter, "Comparison of Methods for Indicating the Measurement Uncertainty of Integral Parameters on the Basis of Spectral Data by Means of the Measurement Uncertainty of the f_1' Value," in *Proceedings of the 2nd CIE Expert Symposium on Measurement Uncertainty*, Braunschweig, Germany, 2006, pp. 159–163.

[27] J.W.T. Walsh, *Photometry Handbook,* 3rd Ed. London, UK: Constable and Robinson Limited, 1958.

[28] G.E. Inman. "Electric Discharge Lamp." U.S. Patent 2 259 040, Oct. 14, 1941.

[29] R.S. Simpson, *Lighting Control, lamp measurement Uncertainty,* 1st Ed. Oxford, UK: Focal Press, 2003.

[30] S.W. Brown, G.P. Eppeldauer, and K.R. Lykke, "NIST facility for spectral irradiance and radiance responsivity calibrations with uniform sources," *Metrologia,* vol. 37, no. 5, pp. 579–582, 2000.

[31] "Diffuser Selection Guide," 2014, http://edmundoptics.com/technical-resources-center/optics/diffuser-selection-guide/.Last accessed on 21 July 2015.

[32] J. Hovila, "New Measurement Standards and Methods for Photometry and Radiometry," Doctoral dissertation, Helsinki University of Technology, 2005.

[33] A.A. Gaertner. Measurement Course on Photometry, Radiometry and Colorimetry. Topic: "LED measurement issues." Institute of National Measurement Standards of the National Research Council of Canada, Ottawa, Canada, Apr. 9–12, 2002.

[34] "Photometers vs Spectrometers: How to Make the Best Choice," 2015, http://www.guided-wave.com/gwi-document-pages/photometer-vs-spectrometer.html. Last accessed on 14 August 2015.

[35] "Photometer or Spectroradiometer? An Estimation of Errors When Using Filter-Based Photometers to Measure the Illuminance of LED Sources," 2009, http://www.pro-lite.co.uk/File/Pro-Lite%20TechNote%20-%20Photometer%20vs%20Spectroradiometer%20for%20LED%20Testing.pdf. Last accessed on 11 July 2015.

[36] S. Sadlak and M. Smith, "Dimming LFL Systems," 2006, http://www.geappliances.com/email/lighting/specifier/2008_07/downloads. Last accessed on 12 July 2015.

[37] S. Park, Y.W. Kim, D.H. Lee, and S.N. Park, "Preparation of a Standard Light-emitting Diode (LED) for Photometric Measurements by Functional Seasoning," *Metrologia*, vol. 43,no.3, pp. 299–305, 2006.

[38] D.H. Lee et al. (2012, July).APMP Supplementary Comparisons of LED Measurements: APMP.PR-S3b Total Luminous Flux of LEDs. Division of Physical Metrology, Korea Research Institute of Standards and Science (KRISS) Daejeon, Rep. Korea. [Online]. Available: http://www.bipm.org.

[39] T.Q. Khan, P. Bodrogi, Q.T. Vinh, and H. Winkler, *LED Lighting: Technology and Perception*, 1st Ed. Berlin, Germany: John Wiley & Sons, 2014.

[40] Y. Ohno, "NIST Publication 250–37," *NIST measurement Services: Photometric Calibrations*, July 1997.

ADDENDUM A: MEASUREMENTS

The following shows different measurement set-ups from the seasoning process up until the verification of the hypothesis. Selected measurements data and plots have been shown in this Appendix.

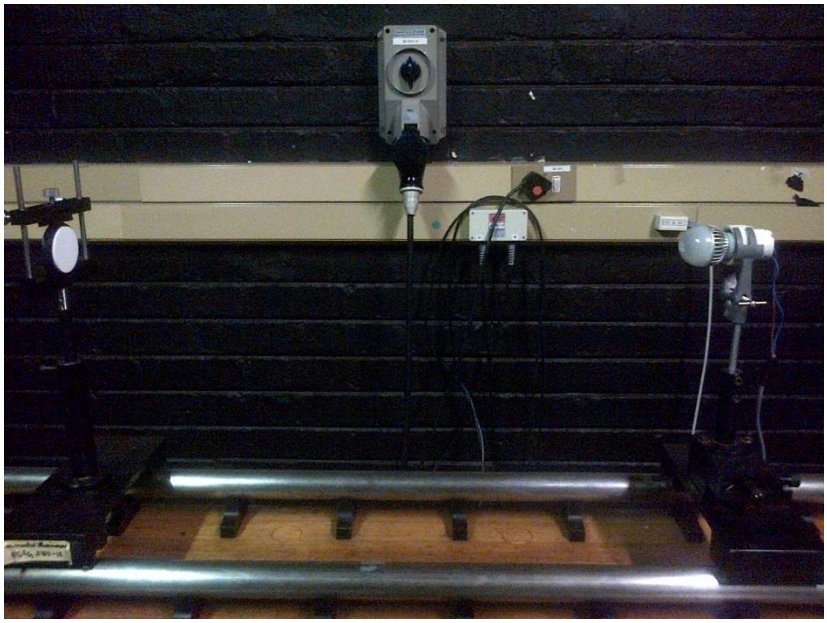

Figure A.1. Intensity measurement set-up for a Pharox 400 lm LED (off state)

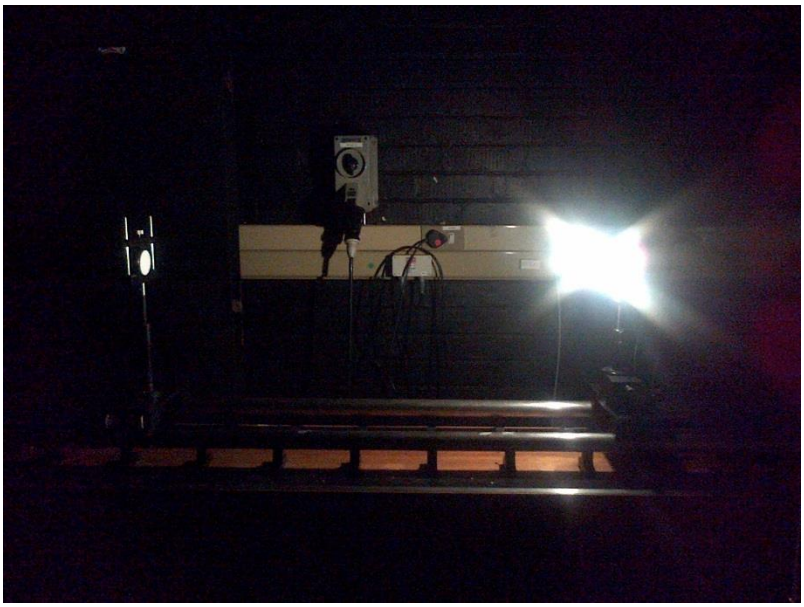

Figure A.2. Intensity measurement set-up of a Pharox 400lm LED (on state)

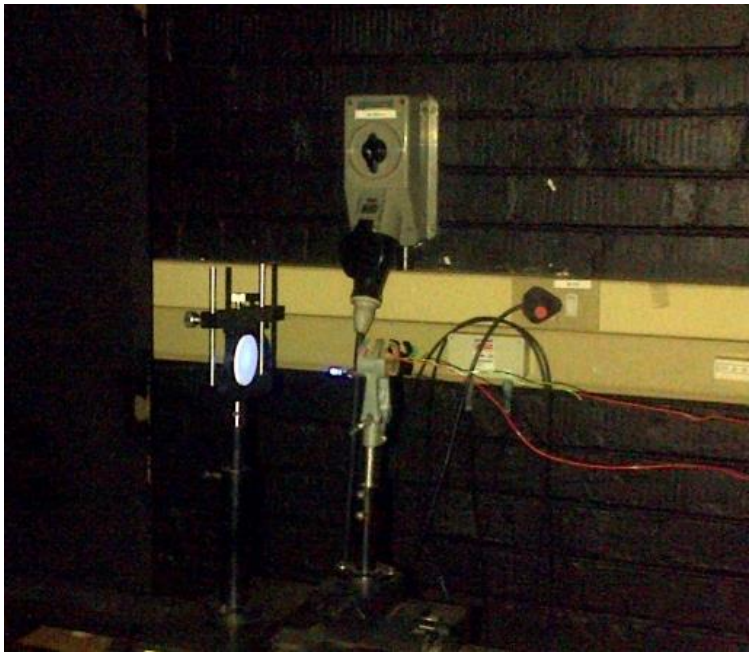

Figure A.3. Intensity and V_j measurement of a blue clear lense 5mm epoxy LED

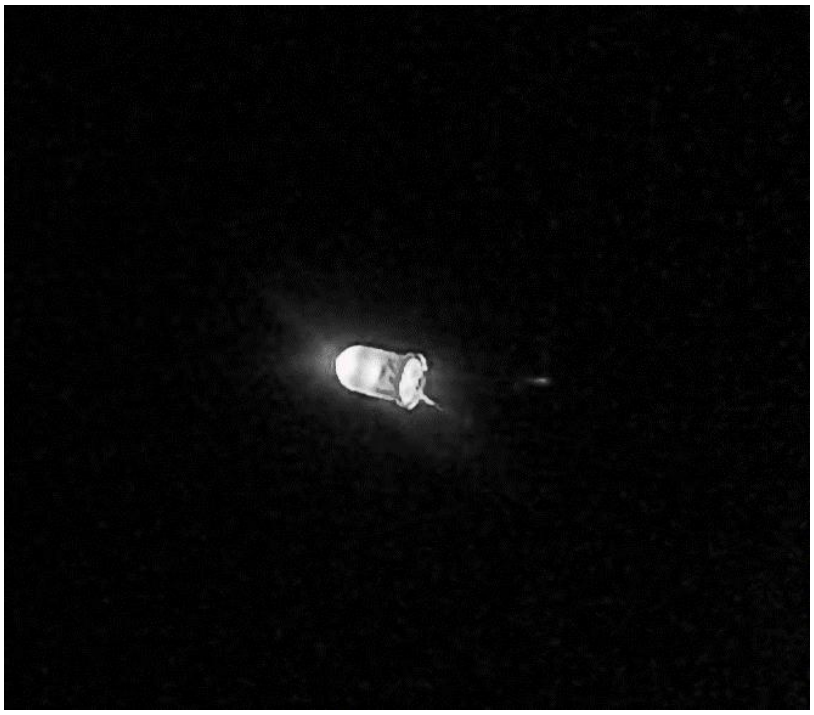

Figure A.4. A 5mm epoxy LED set-up for intensity measurement, showing its complex spatial distribution and back emissions

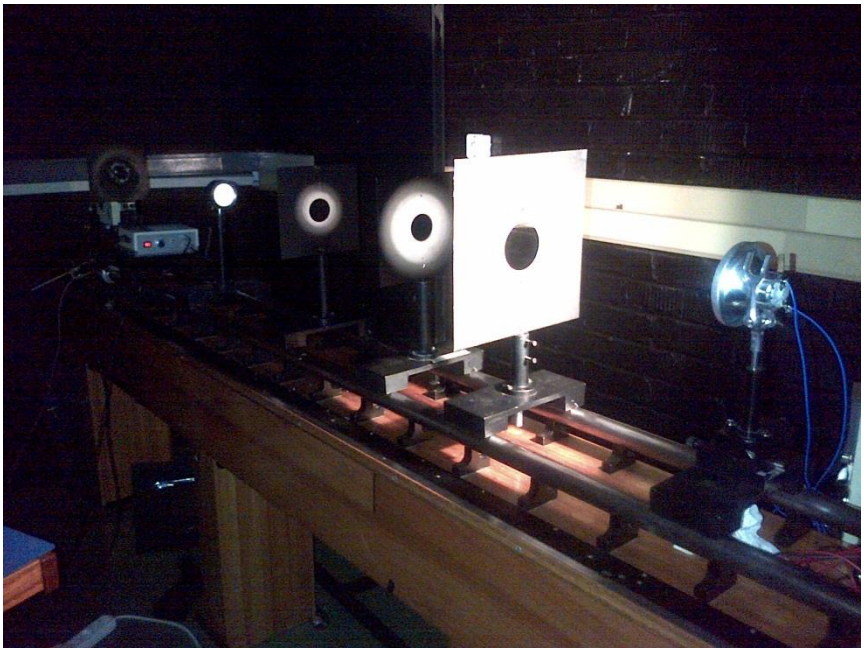

Figure A.5. A more complex set-up including baffles to eliminate reflections from the wall and stray light

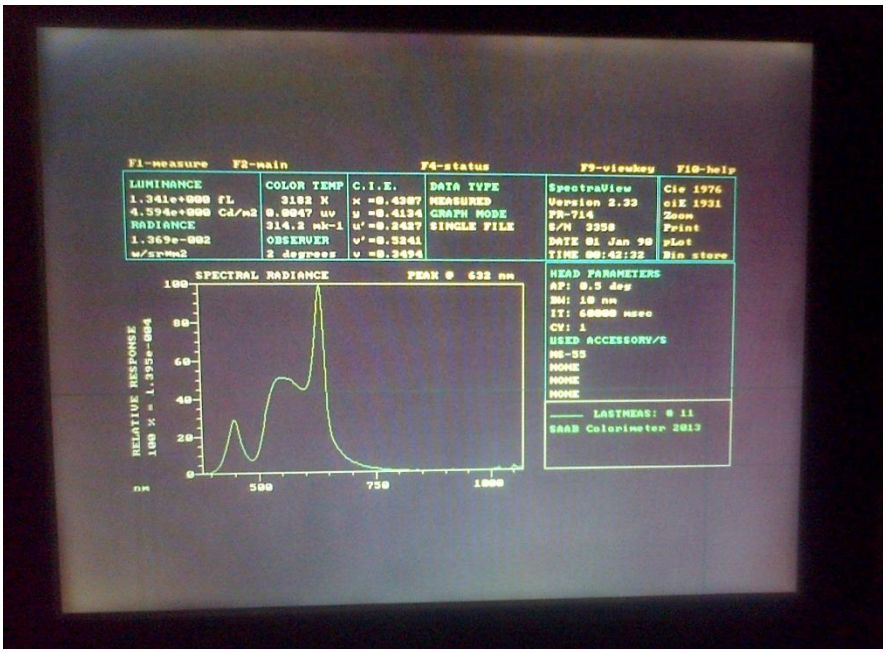

Figure A.6. Spectral radiance (or the SPD) measurement for an RGB LED lamp. Measured using the SpectraScan PR–714

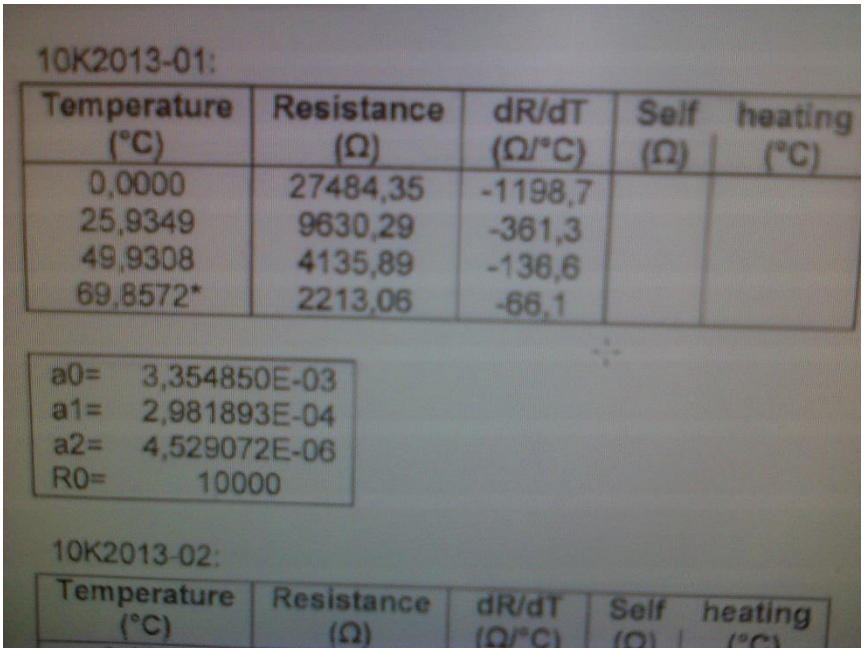

Figure A.7. Calibration data of the thermistor used during the seasoning of LEDs

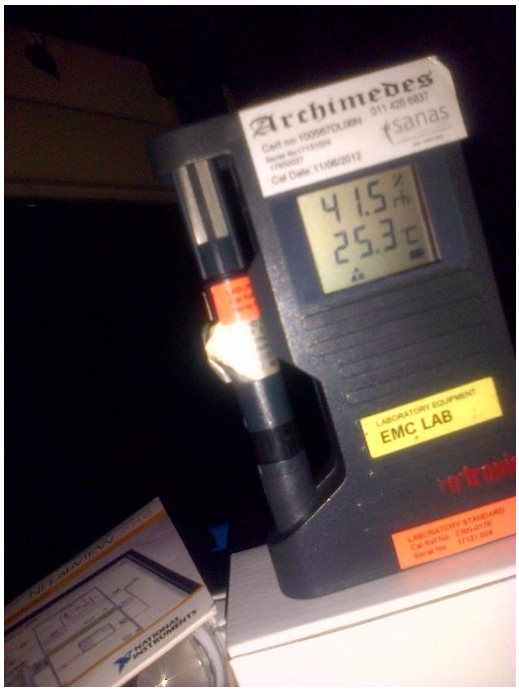

Figure A.8. A calibrated Rotronic thermometer/ hygrometer used to monitor and log the humidity and the ambient temperature inside the laboratory

Figure A.9. Illuminant A lamp and a detector standard used to calibrate the integrating sphere at different distances (d_0)

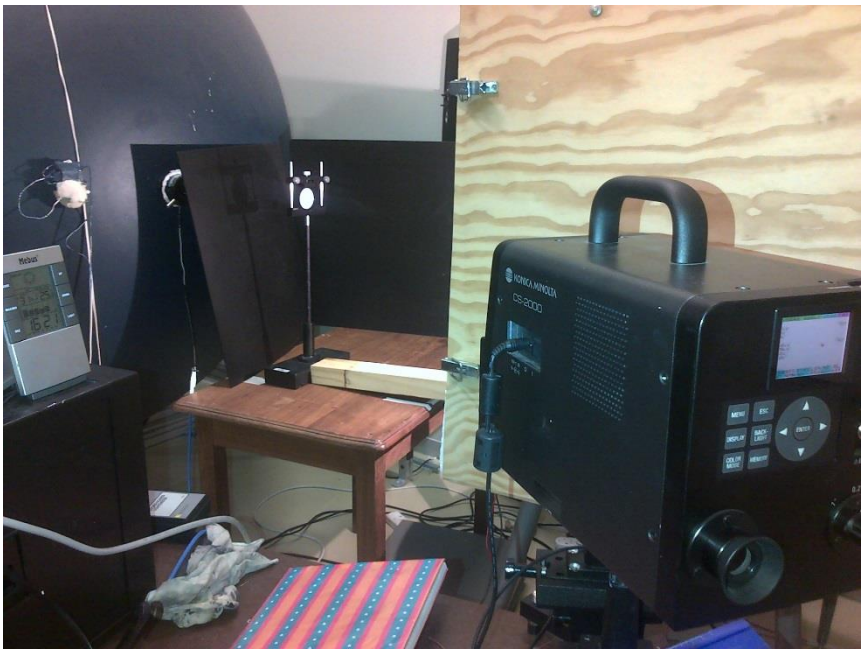

Figure A.10. Measurement set-up used to verify the SPD for illuminant A lamp standard

Figure A.11. Electrical equipment used to power up the lamps

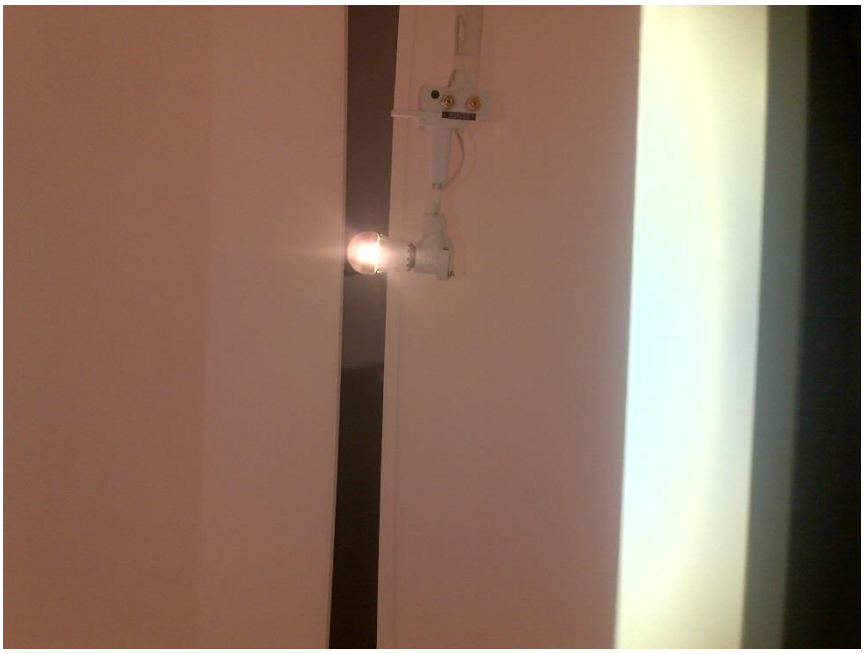

Figure A.12. A warm white Pharox LED lamp total luminous flux measurement using an integrating sphere

Table A.1. Excel spreadsheet used to calculate the correction factor *F* for an LED lamp

Wavelength (λ)	$s_{LED}(\lambda)$	$s_{CAL}(\lambda)$	$s_{REL}(\lambda)$	V(λ)	$s_{LED}(\lambda)*V(\lambda)$	$s_{CAL}(\lambda)*s_{REL}(\lambda)$	$s_{LED}(\lambda)*s_{REL}(\lambda)$	$s_{CAL}*V(\lambda)$
380	0.01113	0.04053						
385	0.018113	0.0451						
390	0.027837	0.050006						
395	0.040398	0.055257						
400	0.055363	0.060859						
405	0.071647	0.066817	0.001	0.001	7.165E-05	6.6817E-05	7.16466E-05	6.682E-05
410	0.087556	0.073137						
415	0.10104	0.079821	0.003	0.002	0.0002021	0.000239463	0.000303121	0.0001596
420	0.110108	0.086873			0	0	0	0
425	0.122154	0.094293	0.007	0.008	0.0009772	0.000660052	0.000855078	0.0007543
430	0.131371	0.102083			0	0	0	0
435	0.140952	0.110241	0.014	0.018	0.0025371	0.001543374	0.001973331	0.0019843
440	0.150892	0.118766						
445	0.161184	0.127654	0.025	0.031	0.0049967	0.003191352	0.004029588	0.0039573
450	0.171817	0.136902			0	0	0	0
455	0.182783	0.146506	0.044	0.050	0.0091392	0.006446257	0.008042472	0.0073253
460	0.194073	0.156458			0	0	0	0

465	0.205673	0.166754	0.073	0.079	0.0162482	0.01217302	0.015014164	0.0131735
470	0.217574	0.177384			0			
475	0.229763	0.188341	0.106	0.120	0.0275715	0.019964185	0.024354852	0.022601
480	0.242226	0.199616			0	0	0	0
485	0.25495	0.2112	0.175	0.177	0.0451262	0.036960029	0.044616306	0.0373824
490	0.267922	0.223081				0	0	0
495	0.281127	0.235249	0.265	0.273	0.0767477	0.062341092	0.07449865	0.0642231
500	0.29455	0.247693			0			
505	0.308177	0.260399	0.399	0.420	0.1294345	0.103899319	0.122962762	0.1093677
510	0.321993	0.273357			0	0	0	0
515	0.335982	0.286552	0.624	0.638	0.2143563	0.178808565	0.209652563	0.1828203
520	0.350128	0.299973				0	0	0
525	0.364418	0.313604	0.783	0.790	0.2878899	0.245552105	0.285339017	0.2477473
530	0.378834	0.327434			0			
535	0.393362	0.341447	0.914	0.928	0.36504	0.312082922	0.359532886	0.3168632
540	0.407986	0.35563				0	0	0
545	0.422692	0.36997	0.987	0.982	0.4150836	0.365159983	0.41719708	0.3633101
550	0.437464	0.38445			0	0	0	0
555	0.452287	0.399058	1.000	1.000	0.452287	0.399057826	0.452286953	0.3990578
560	0.467147	0.413779			0			

565	0.482029	0.4286	0.983	0.981	0.4728702	0.421314186	0.473834283	0.420457
570	0.496919	0.443505				0	0	0
575	0.511804	0.458479	0.903	0.905	0.4631823	0.414006865	0.462158678	0.4149238
580	0.526669	0.473512			0	0	0	0
585	0.541502	0.48859	0.805	0.806	0.4364509	0.393314989	0.435909441	0.3938036
590	0.556291	0.503697			0			
595	0.571021	0.518821	0.691	0.695	0.3968599	0.358505125	0.394575824	0.3605804
600	0.585683	0.533953			0	0	0	0
605	0.600263	0.549072	0.557	0.563	0.3379481	0.30583316	0.33434653	0.3091276
610	0.614751	0.564171			0	0	0	0
615	0.629136	0.579241	0.441	0.450	0.2831112	0.255445156	0.27744895	0.2606583
620	0.643407	0.594261						
625	0.657555	0.609227	0.319	0.323	0.2123904	0.194343499	0.209760167	0.1967804
630	0.67157	0.624127			0	0	0	0
635	0.685444	0.638949	0.209	0.213	0.1459995	0.133540341	0.143257694	0.1360961
640	0.699166	0.653684			0	0	0	0
645	0.712729	0.668319	0.137	0.140	0.0997821	0.091559706	0.097643916	0.0935647
650	0.726126	0.682851						
655	0.739349	0.697259	0.081	0.080	0.0591479	0.056477956	0.059887239	0.0557807
660	0.75239	0.711546			0	0	0	0

665	0.765244	0.725698			0			
670	0.777904	0.739708	0.035	0.032	0.0248929	0.02588979	0.027226648	0.0236707
675	0.790365	0.753566			0	0	0	0
680	0.779954	0.767266			0			
685	0.715721	0.780805	0.013	0.012	0.0085887	0.010150462	0.009304375	0.0093697
690	0.620206	0.79417			0	0	0	0
695	0.50751	0.807357			0			
700	0.392166	0.820362				0	0	0
705	0.286162	0.833181	0.004	0.003	0.0008585	0.003332724	0.001144647	0.0024995
710	0.197183	0.845801			0			
715	0.128306	0.858223			0	0	0	0
720	0.078838	0.870446			0	0	0	0
725	0.045745	0.882458			0			
730	0.025065	0.894259	0.001	0.001	2.507E-05	0.000894259	2.50653E-05	0.0008943
735	0.012969	0.905845						
740	0.006337	0.917211						
745	0.002924	0.928358						
750	0.001274	0.939278			4.9898165	4.412754579	4.947253928	4.449001
755	0.000524	0.949974						
760	0.000204	0.960443						

765	7.47E-05	0.97068						
770	2.59E-05	0.980689						
775	8.47E-06	0.990462		***F***	**1.0003861**			
780	2.62E-06	1						

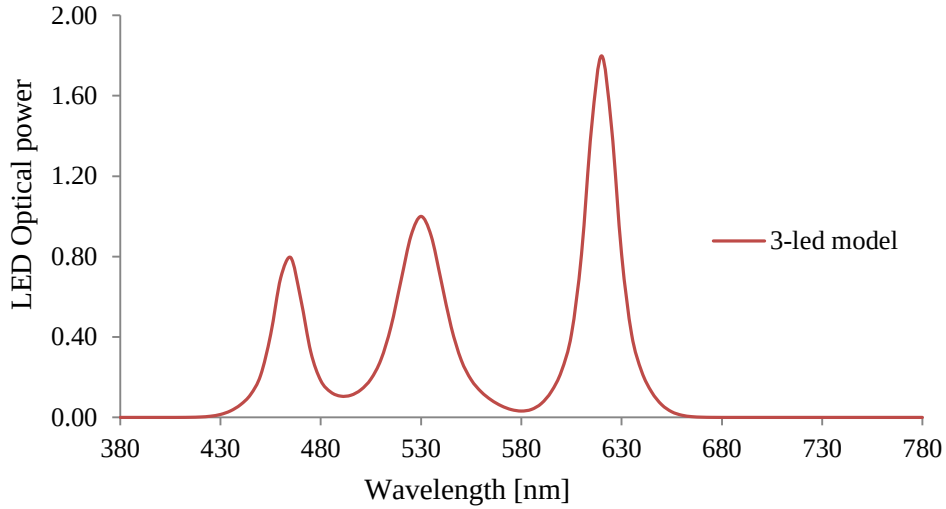

Figure A.13. A 3–LED model (RGB) model which performed poorly in terms of temperature stability and CRI